LUND UNIVERSITY

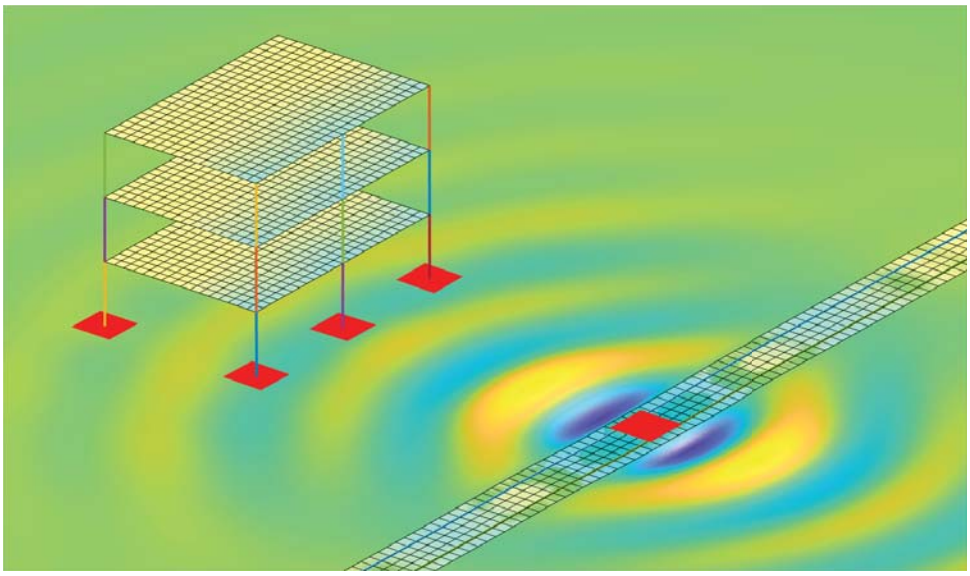

PARAMETER STUDY OF RAILWAY-INDUCED STRUCTURAL VIBRATIONS USING NUMERICAL AND SEMI-ANALYTICAL MODELS

FILIP RASMUSSEN

Structural Mechanics

Master's Dissertation

DEPARTMENT OF CONSTRUCTION SCIENCES

DIVISION OF STRUCTURAL MECHANICS

ISRN LUTVDG/TVSM--24/5268--SE (1-60) | ISSN 0281-6679

MASTER'S DISSERTATION

PARAMETER STUDY OF RAILWAY-INDUCED STRUCTURAL VIBRATIONS USING NUMERICAL AND SEMI-ANALYTICAL MODELS

FILIP RASMUSSEN

Supervisor: **PETER PERSSON**, Associate Professor, Division of Structural Mechanics, LTH.
Assistant Supervisor: Professor **LARS VABBERSGAARD ANDERSEN**, Aarhus University.

Examiner: Professor, **KENT PERSSON**, Division of Structural Mechanics, LTH.

Printed by V-husets tryckeri LTH, Lund, Sweden, July 2024 *(P1)*.

For information, address:
Division of Structural Mechanics,
Faculty of Engineering LTH, Lund University, Box 118, SE-221 00 Lund, Sweden.

Homepage: www.byggmek.lth.se

Abstract

As the importance of sustainability increases more weight is laid upon using both greener building materials and efficient transportation systems. As more and more buildings are being built with wood and other light weight materials, and ever more slender constructions, the need to understand the impact of vibrations in these types of structures increases. Furthermore the increasing urban density leads to more buildings being built near railways, and there is apprehension within the industry to constructing these potentially vibration sensitive building near railways. These vibration can have an impact on both occupants' health and the function of sensitive equipment within the buildings. The solution has been to construct concrete buildings as their heavier weight and stiffer construction are assumed to counteract the impact of railway vibrations. However, discounting the wooden buildings is often done without knowledge about if these buildings actually are worse at handling vibrations than concrete buildings.

In this master's dissertation, the behavior of wooden and concrete structures when exposed to external vibrations is examined. Through the use of a new three dimensional semi-analytical soil model an extensive parameter study was conducted for both a steady state stationary load and a realistic train load. The soil model was coupled to a finite element structure and building, soil and train parameters were studied. By examining comfort vibrations inside the building within a frequency spectrum of 1 to 80 Hz, the impact of each variable could be determined and comparisons between similar concrete and wooden structures could be made.

The parameter studies showed that a correlation between the natural frequency of the building and the large response frequency in the soil did not seem to cause any additional resonance in the building. It was also discovered that increased structural damping of a building can cause a large increase in vibrations within a building exposed to an external vibration. A comparison between examining steady state conditions and a realistic train load showed that while results of a steady state analysis may indicate how the building will react to a train load, the effect of a parameter change in the steady state analysis does not always correlate to the effect of that same parameter change when considering a train load. When comparing the wooden and concrete buildings to each other, it was found that while for most scenarios the concrete building has the lowest vibration levels, there are some exceptions to that rule. Those exceptions were when the building was placed on very elastic soil such as clay, when the structural damping of the two buildings was similar, and when the building is placed within approximately 20 meters of the railway.

Preface

This dissertation concludes my long studies at the Faculty of Engineering (LTH) at Lund University. This work was conducted at the Division of Structural Mechanics. I would like to thank my supervisor Dr. Peter Persson for both the initial idea for this dissertation as well as his continued support, enthusiasm and fruitful discussions during the many work hours spent on this dissertation. I would further like to thank my assistant supervisor Prof. Lars Vabbersgaard Andersen at Aarhus University for his help with both getting the program running and analyzing the results. I would also like to thank Paulius Bucinskas, PhD, for creating and providing both programs used in this work, as well as taking time out of his days to help me hunt down bugs and understanding the programs.

Lastly, I would like to thank my friends and family for their support throughout my life. A special thanks to my mother Veronica Parada, my brother Marcelo Walter, Janos Walter and of course my lovely girlfriend Hanna Begander.

Filip Rasmussen, Lund, April 2024

Abbreviations

VC - Vibration criterion
RMS - Root mean square
FE - Finite element
BEM - Boundary element method
PDE - Partial differential equation
DOF - Degree of freedom
SDOF - Single degree of freedom
MDOF - Multi-degree of freedom
P-wave - Primary wave
S-wave - Secondary wave
R-wave - Rayleigh wave
SV-wave - Secondary vertical wave
PSD - Power spectral density
FOR - Frame of reference
SSI - Soil structure interaction
CLT - Cross laminated timber

Contents

1 Introduction

1.1 Background

Vibrations in buildings have become a more important factor to consider when constructing buildings using new techniques, less materials and in a denser urban environment. This leads to more slender constructions that can be more exposed to and sensitive to vibrations. Also, more and more buildings are made of wood in order to create a more sustainable society and to reduce CO_2-emissions. But wooden buildings are met with resistance in the industry as there are still knowledge gaps about their functions, such as in regards to railway-induced vibrations. In order to investigate the vibration levels in buildings there is a need for detailed computer models that can account for the vibrations sources, the soil in which the vibrations propagate, the soil-structure interaction and the dynamic behavior of the buildings. These models are often very demanding in terms of time and computational requirements, which leads to them not often being used in early stages of a building project. Then, when the choice between wooden buildings and concrete buildings is made it can become easy to choose the material with the largest knowledge base, especially for buildings in vibration exposed situations, such as near railway lines. With more comprehensive knowledge of how wooden buildings and concrete buildings behave dynamically in relation to each other, the materials can compete on equal terms.

1.2 Previous studies

The subject of vibrations in structures from external sources has been studied using several different methods. A common approach is to use the finite element (FE) method in three dimensions when modeling both the soil and structures. In Torndahl and Svensson [1] a parameter study was conducted on a simplified building structure using a reduced FE model. The steady state response of the building was examined. In Persson and Andersen [2] the effect of varying the slab thickness of a simplified light- and heavy-weight building was analyzed using a reduced FE model. The steady state response of the building was examined. In Negreira Montero [3] the effect of external vibrations on an underground facility was investigated using a FE model. The response to a bus load, a road traffic load and a walking load was examined.

Another modeling approach is to use the FE method in two dimensions using plane stress elements in order to examine the system. Johansson [4] examines the effect surrounding buildings and building properties can have on measured vibration levels. The steady state response of the building was examined. Persson et al. [5] conducted a parameter study on the effect of soil and concrete slab parameters on a slab on soil. The steady state response of the slab was examined.

There are also other approaches that are used, such as using the boundary element method (BEM) combined with the FE-method and examining the structures using so called 2.5D FEM models which properties are invariant along one axis, while still providing a 3D response. There also exists some semi-analytical approaches. Villot et al. [6] used a BEM / FEM model in both 2D and 2.5D to investigate the influence of different building parameters on the building response. The response to train-induced vibrations was examined. Malmborg et al. [7] used a 2.5D model to establish the free-field ground vibrations from railway traffic and then applied these vibrations on a 3D building model. The effect of differing train speeds on a light- and heavy-weight building was examined. Tao et al. [8] used a semi-analytical model to examine the effect of railway vibrations on buildings with pile foundations.

1.3 Aim and methods

This masters dissertation aims to improve knowledge of the dynamic behavior of wooden and concrete buildings exposed to railway-induced comfort vibrations. By performing a parameter study on the soil conditions, materials, structural dimensions and sources, a greater knowledge about what design choices impact the comfort vibrations inside a building will be gained. The primary research questions studied are as follows:

- What parameters of a railway, soil and building system have a significant effect on vibration levels in a building, and what effect do they have?
- How does a wooden building compare to a similar concrete building when exposed to railway-induced vibrations?
- How does a steady state analysis of a stationary load compare to examining a moving train load?

The analysis was done through the use of a semi-analytical soil model and a finite element building model, using stationary loads in a fixed frame of reference and moving railway-loads in a mixed frame of reference.

1.4 Limitations

The master's dissertation is limited to examining comfort vibrations in buildings and train speeds below the critical speed of wave propagation in soil. The models examined are simplified. In the case of the building model, only the load bearing elements are considered, and for the moving load case, the train model only contains one vehicle.

2 Structural building vibrations

When examining externally induced building vibrations, there are three major parts that need examination. These parts are the *source* of the vibration, the *medium* trough which the vibrations travel and the *receiver* where the level of vibrations are evaluated.

2.1 Sources

External vibrations in a urban environment can originate from many different sources. While earthquakes are an important factor to consider in many environments, in a Nordic context they are both rare and not very powerful. Instead it is the man-made sources that are often the most important to take into account. The most common external vibration causes are construction (e.g. pile driving), heavy road traffic and railways. This dissertation is concerned with vibrations from railways.

2.2 Medium

The medium can describe ground that the vibration waves travel through, bridges and tunnels as well as potential obstacles that can affect the wave propagation. When modeling the ground it is important to consider the stratification of the soil, the existence of and distance to bedrock and the properties of these elements. Man made elements such as roads, sidewalks, ditches and foundations can also have a considerable impact on the wave propagation.

2.3 Receiver

The receiver is in most cases a building, but can also be other vibration sensitive structures, such as tunnels or bridges. Vibrations within buildings does not depend only on the impinging vibration waves, but also on the elements of the structure itself, such as its design, materials and furnishings [9]. Concerns with vibrations in buildings can stem from the need to keep vibration sensitive equipment in working order and keeping residents and workers from experiencing discomfort. The frequencies associated with whole body vibrations are in the 1-80 Hz range [10], while structural noise caused by vibrations is generally found in the 20-200 Hz range [11]. There exists a significant overlap between the two types of disturbances, and residents may have difficulty differentiating between the two when reporting a disturbance.

There is also the concern with structural damage caused by railway traffic, such as minor cosmetic damage and more serious structural damage to buildings. However,

these fears are almost always misattributed. The vibrations caused by railway traffic are not large enough to cause even minor cosmetic damage to most buildings, given reasonable build quality and reasonable distance to the train track [11]. Instead, there are often far more credible causes of cosmetic damage in buildings close to railways. These causes can include settlement, temperature variation, aging of building materials and moisture issues. Some damage may also be caused by the construction of new railways, when utilizing techniques such as pile and sheet driving, and can then later be incorrectly attributed to the new railway traffic [11].

2.4 Evaluation of vibrations

Several standards have been devised to evaluate the effect of vibrations on human occupancy. The international standard ISO 2631 [12] utilizes the root-mean-square (RMS) of the velocity amplitude to create an effective value that allows for comparisons and specification of guidelines. RMS is also used in the so called Vibration Criterion (VC) curves that can be used by equipment manufacturers to specify acceptable vibration levels.

3 Governing theory

The computational model used in this dissertation consists of a finite element model coupled to a semi-analytical soil model. This model can be used with a fixed frame of reference or a mixed frame of reference in order to account for a moving load. An overview of the governing theory for each part is presented in this chapter.

3.1 The finite element method

The structural modeling in this dissertation uses the finite element method. The FE method is a common numerical method for modeling of structures. Its main advantages are its flexibility for modeling complex geometry and behavior and the widespread availability of commercial software. It works by approximating solutions to partial differential equations (PDEs) derived from balance equations. These PDEs are most often too complex to be solved analytically and the problem is therefore divided into smaller elements, or finite elements. Each element contains a number of nodes which define the shape of the element. The collection of all elements is called a mesh. The variation of the sought field variables (such as displacements) between nodes in an element are chosen by an approximating function, known as the shape function, and the field variables are discretized in each node. The shape function is often a linear or a polynomial function. Each node can be associated with variables called degrees-of-freedom (DOF). These DoFs can represent variables such as the displacement of a node in several directions when analyzing a structural problem. By using a denser mesh of elements, the accuracy of the method generally increases and it can be shown to typically converge towards the exact solution.

3.2 Fundamental structural dynamics

When structures are exposed to changes in displacements and forces over time, a static analysis may not be applicable. The dynamic loads can for example be wind loads, footfalls and rail traffic and earthquakes. To analyze a dynamic system, a simple system consisting of a mass m connected to a spring with the stiffness k and a damper with a damping coefficient c that is exposed to a periodic load *f(t)*, as seen in Figure 3.1, is considered.

This system can be seen as having a single degree of freedom (SDOF), the displacement u. By applying Newton's second law of motion $f = m\ddot{u}$, this SDOF system can be described by

$$m\ddot{u} + c\dot{u} + ku = f(t). \tag{3.1}$$

where a dot over the displacement indicates the time derivative, with one dot meaning

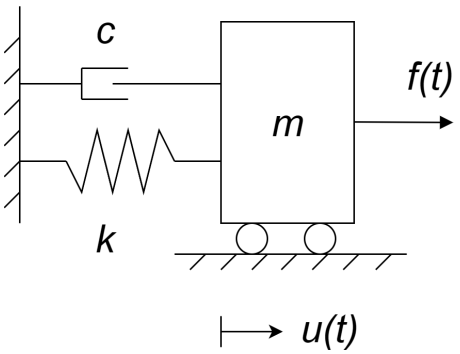

Figure 3.1: A single degree of freedom system.

velocity and two dots denoting acceleration. This relation can be expanded to apply to a multi-degree of freedom (MDOF) system. Here, the mass, stiffness and damping are represented by matrices of $n \times n$ size where n is the number of DOFs, while the forces and the displacement and its derivatives are vectors of size $n \times 1$. The equation for motion then becomes

$$\mathbf{M\ddot{u}} + \mathbf{C\dot{u}} + \mathbf{Ku} = \mathbf{f}(t). \tag{3.2}$$

3.2.1 Steady state dynamics

When a system is exposed to a harmonic load, the response of the system becomes periodic after an initial transient response. This is known as a steady state response. By using complex analysis of the SDOF equation of motion, the steady state response can be defined as a displacement amplitude and a phase angle which describes the offset of the harmonic response to the harmonic load. The steady state amplitude for a SDOF system is calculated as

$$u_0 = \frac{p_0}{\sqrt{(k - \omega^2 m)^2 + \omega^2 c^2}} \tag{3.3}$$

where u_0 is the displacement amplitude, p_0 is the force amplitude and ω is the angular frequency of the harmonic load. A similar solution exists for a MDOF system, where the complex displacement amplitude for each DOF can be solved using a system of linear equations:

$$(-\omega^2\mathbf{M} + i\omega\mathbf{C} + \mathbf{K})\mathbf{u^*} = \mathbf{p}_0. \tag{3.4}$$

Here, $\mathbf{u^*}$ is the complex displacement vector and $\mathbf{p}_0$ is the force amplitude vector. Using $\mathbf{u^*}$, the phase angle θ for a single DOF u_j^* can be determined as

$$\theta = arg(u_j^*). \tag{3.5}$$

By using the derivative of the displacement amplitude, the velocity amplitude can be evaluated instead. For this dissertation, the steady state velocity amplitude is the primarily evaluated variable.

3.2.2 Resonance

When a SDOF structure is released from deformation and allowed to vibrate freely, the frequency at which it vibrates is known as its natural frequency. For a damped

SDOF system, the natural frequency can be calculated as

$$\omega_n = \sqrt{\frac{k}{m}\left(1 - \left(\frac{\eta}{2}\right)^2\right)} \tag{3.6}$$

where ω_n is the natural angular frequency and η is the structural loss factor of the system. The relationship between η and c for at a resonant frequency in a SDOF system is described by

$$\eta \approx \frac{c}{m\omega_n}. \tag{3.7}$$

For a MDOF system, there exists multiple natural frequencies, depending on the shape of the initial deformation. These shapes are known as eigenmodes. For a undamped MDOF system with no load applied, the equation of motion can be rewritten as a eigenvalue problem

$$(\mathbf{K} - \omega^2\mathbf{M})\mathbf{\Phi} = 0 \tag{3.8}$$

where $\mathbf{\Phi}$ is a eigenvector. This eigenproblem has the trivial solution

$$det(\mathbf{K} - \omega^2\mathbf{M}) = 0. \tag{3.9}$$

Solving for ω gives n number of natural frequencies ω_n, where n is the number of DOFs in the MDOF system. Inserting any natural frequency ω_n in Equation 3.8 gives a unique eigenvector, which corresponds to the displacement of each node in the corresponding mode shape. In reality, a structure has an infinite number of natural frequencies and corresponding modes, but it is common to only consider the first few modes when examining a structure's dynamic behavior.

When a undamped system is excited by a harmonic load that matches a natural frequency, the response of the system tends towards infinity. However, all real systems contains some damping. When damping is introduced, the response of a system with the same conditions can be several times higher than for harmonic loads not matching a natural frequency.

3.3 Fundamental soil dynamics

In modeling the ground, several assumptions can be established. When considering vibrations with small amplitudes and with a source that is moving slower than the wave speed of the soil, the soil can be considered to be a homogeneous material with linear elastic properties. This allows for simpler formulations when creating a computational model. The vibrations within the soil can be shown to consist of several different types of waves moving independently. The primary wave (P-wave) consists of the compression of the soil granulate, and is the fastest moving wave type. The secondary wave (S-wave) consists of the soil granulate moving perpendicular to the wave propagation direction, as shear deformation. While slower moving, the S-wave generally contains more energy than the P-wave, and is thus more important to consider when examining traffic vibrations [13]. When considering a free surface of the soil, the interaction of the P- and S-waves with the surface creates another wave type, known as the Rayleigh-wave (R-wave). The R-wave travels close to the surface, with

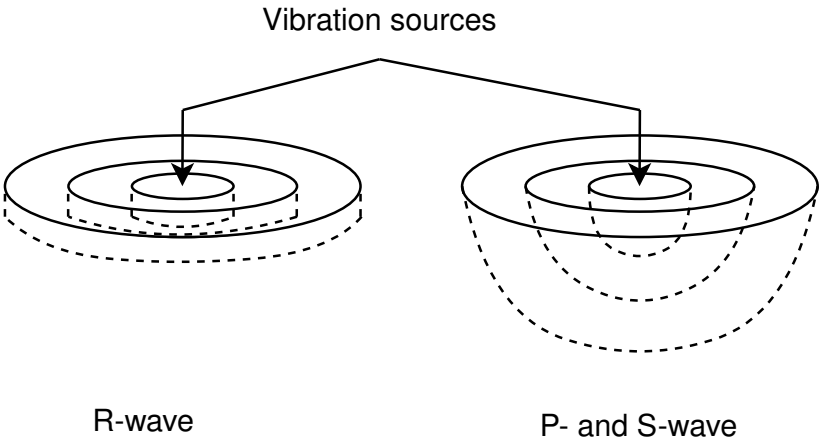

Figure 3.2: The geometric wave expansion for R-, P- and S-waves in a soil.

the particles moving in a elliptical shape with larger amplitudes near the surface and reducing with depth. It moves slower than the S-wave, but with more energy thus making it the most influential wave type to consider when a free surface is involved. There also exists other types of waves such as the Love-wave, however their effect on structures above ground are small. [14]

When considering the impact of the different types of waves, damping must be accounted for. Geometric damping occurs as the wave spreads out over a larger area as the distance from the source increases. As P- and S-waves propagate throughout the entire soil medium, the geometric damping on these waves is larger than for the R-waves, which only propagates near the surface of the soil. This means that the P- and S-waves propagates through an expanding half sphere from the origin, while the R-wave only propagates trough an expanding cylinder with a fixed height near the surface, which limits the amount of material in which damping may occur, see Figure 3.2. Material damping occurs due to energy losses to e.g. heat. Damping can be both frequency dependent and independent, based on the type of damping model chosen.

3.4 Semi-analytical soil model

The computational soil model used was developed by Bucinskas [13]. It is able to calculate the wave propagation in a horizontally stratified medium. The formulation allows for semi-infinite layers (half-spaces) and has no boundary reflections, which allows the geometry of the examined model to remain small. Using the so called Green's function, which is used to solve differential equations, it is able to calculate the displacement and velocity amplitudes of the system, and utilizes a method by Thomson [15] and Haskell [16] to acquire the Green's function. By using a so called transfer matrix the displacements and traction can propagate through one soil layer, and then the layer transfer matrix is used to assemble a global transfer matrix for all layers which can be used to obtain the Green's function. To overcome stability issues with this method, the orthonormalization method by Wang [17] is utilized. This method uncouples the P-wave and the vertical secondary (SV) waves before

propagating them through a layer, as well as dividing thick layers into smaller ones in order to eliminate exponential terms which can grow beyond the capability of floating point numbers when using thick layers or high frequencies. By using these techniques the matrix calculations uses matrix dimension no larger than 6 x 6, which allows for efficient computations.

In order to include structures into the model, the model uses soil-structure interaction (SSI) nodes. These nodes allow for coupling of the soil model to rigid blocks, piles, cavities and FE models. The program used to analyze the fixed frame of reference model is freely available to download in [13] and is called *GCity*. A user guide for the program is also available with the download. A modified version of the available GCity_3.0.3 was used in this dissertation. For a more detailed description of the model, see [13].

3.5 Mixed-frame-of-reference model

To account for a moving train load, a mixed-frame-of-reference computational model was utilized. The computational model was developed and provided by Bucinskas [18] and is named *SubGCity*. A comprehensive description of the model can be seen in [19].

3.5.1 Governing equation

The model is divided into two frames of reference (FOR), a fixed FOR for the soil and structure modeling and a moving FOR for the railway vehicle and track. By formulating the displacements of the fixed FOR in the moving FOR and vice versa, the two parts can be combined into one mixed FOR. By the use of this formulation, a governing equation of the mixed FOR system can be established as

$$\tilde{\mathbf{K}}(\omega_m, \omega_f)\tilde{\mathbf{U}}(\omega_m, \omega_f) = \tilde{\mathbf{F}}(\omega_m, \omega_f) \tag{3.10}$$

where $\tilde{\mathbf{K}}(\omega_m, \omega_f)$ is the stiffness matrix of the system, $\tilde{\mathbf{U}}(\omega_m, \omega_f)$ is the displacements of the vehicle, global railway tack-soil system and FE structure, $\tilde{\mathbf{F}}(\omega_m, \omega_f)$ represents the coupling of the vehicle and rail as well as the displacements of the wheels and ω_f and ω_m represents the considered angular frequencies in the fixed and moving FOR respectively. After solving the system for a unit track unevenness, the actual track unevenness can be applied and the displacement of the FE system in the fixed FOR can be determined.

3.5.2 Railway and vehicle

To account for the train vehicle moving over the rail, *SubGCity* utilizes a railway track that is two-dimensional and only considers vertical wheel-rail interaction forces. The program utilizes a model described by Sheng et al. [20]. Here, the railway is composed of rails, rail pads, sleepers and ballast in layers. The rails are modelled as Euler beams,

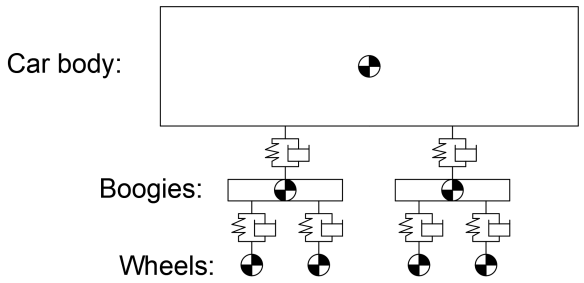

Figure 3.3: Illustrative image of the vehicle model showing the connections of the rigid bars and masses with springs and dampers.

which are connected to rail pads which are modelled as distributed vertical springs. These are then connected to sleepers which are represented as a distributed mass, and the sleepers are finally connected to the ballast which is modelled as a viscoelastic layer with a mass and stiffness. This system can then be coupled to the soil model.

The vehicle that runs along the track is a 10-DOF model consisting of wheels, boogies and a car body. These are then connected by springs and dampers as seen in Figure 3.3. The boogies and car body are modeled as rigid bars with mass and moment of inertia, and the wheels are modeled as lumped masses. The masses have a total of 7 vertical displacement DOF:s, and the rigid bars have a total of 3 rotational DoF:s. [21]

To connect the vehicle to the railway with accurate interaction, Hertzian springs are used. This is a type of spring that are commonly used in contacts mechanics in order to describe the interaction and deformation of two elastic objects in contact [22].

3.5.3 Track unevenness

The track unevenness is the largest contributor of higher frequency vibration [19] and is therefore important to model accurately. In this mixed FOR model the track unevenness is described through the use of power spectral density (PSD) functions. These are functions that can be used to describe the magnitude of the irregularities of a rail as a function of the spatial frequencies. The PSD functions are generally derived from field measurements, and different railway authorities uses different PSD functions to describe the roughness of railway tracks. [21] As noted in Chapter 3.5.1, the track unevenness is not needed to solve the governing equation of the mixed FOR model as this can be done with a unit unevenness, and the actual unevenness can instead be applied after the solving of the displacement vectors.

3.6 Root mean square value

As discussed in Chapter 2.4, a common way to evaluate vibrations is through the use of RMS values. A RMS value is a way to define a single value to represent a discrete set of values. As compared to a mean value, the RMS value does not account for the

sign of the values, and has a higher weighting of the peaks of the evaluated values. This is useful when examining waveforms such as those caused by vibrations. For a discrete signal of the quantity x, the RMS of the quantity is calculated as

$$x_{RMS} = \sqrt{\frac{1}{n}(x_1^2 + x_2^2 + ... + x_n^2)} \tag{3.11}$$

where n is the number of discrete points in the signal.

4 Model Description

The examination of the soil-building system was divided into two parameter studies. The first examined how an oscillating stationary vertical load affected the vibration levels inside the building, by varying a range of parameters. This parameter study used the *GCity* program. The second parameter study examined how a realistic moving train load affected the vibration levels. This study used the more computationally costly *SubGCity* program and examined the parameters which were shown to have a significant effect on the vibration levels in the first parameter study.

4.1 Finite element building model

In order to have a reference case for the parameter studies, a simple building structure was assembled. The decision was made to use a pillar-beam structure with one-way spanning floor plates. The pillars are situated on completely rigid surface footings, which in turn are coupled to the soil. Only the structural elements were modelled, i.e., non-load bearing structures were not explicitly modeled.

Two standard building cases were constructed, one with wooden structural elements and one with concrete elements. The overall layout of both buildings are identical, with minor differences in the dimensions of the structural elements (c.f. Tables 4.6 and 4.7, and can be seen in Figure 4.1.

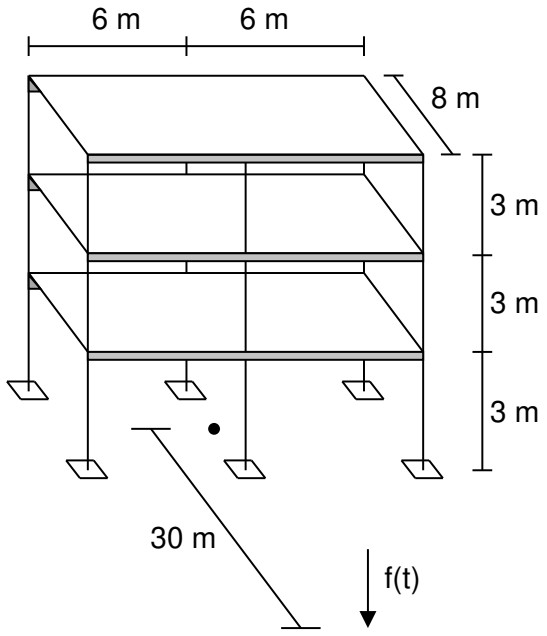

Figure 4.1: The standard case of the building model. The dot represents the center point of the building on the ground surface.

The span of the side of the building containing a center pillar is hereafter referred to as the length of the building, and the side with no center pillar is referred to as the width of the building. The dimensions of the building and its elements can be seen in Table 4.1.

Table 4.1: Properties of the building model for the standard case.

Property	Wooden building	Concrete building
Building width (m)	8	8
Building length (m)	12	12
Floor height (m)	3	3
Pillar cross section (m)	0.16 x 0.16	0.2 x 0.2
Beam cross section (m)	0.115 x 0.360	0.2 x 0.4
Floor plate thickness (m)	0.280 (7 layers of 0.040)	0.3

The wooden building is constructed using cross-laminated-timber (CLT) floor plates and glulam beams and pillars. The CLT plates use seven layers of wood with the outer layers being oriented in the span direction and the other layers alternating between 0 degrees from span direction and 90 degrees from span direction. The concrete building is constructed by reinforced concrete, however, reinforcement is not explicitly modeled because the deformations considered are small and the study only examines the elastic response of the concrete. In these conditions the rebar is not active and will therefore not affect the stiffness of the concrete structure. The material properties of the wood and concrete can be seen in Table 4.2. As timber is a orthotropic material, it has different element properties in different directions. E_1 and E_2 represents the Young's modulus in the fiber direction and perpendicular to the fiber direction, respectively For the shell elements used in the floor plates, the elastic properties in the thickness direction of the elements are not considered. G_{ij} represents the shear modulus in the ij plane.

Table 4.2: The material properties used in the standard cases.

Property	Wood	Concrete
Density (kg/m^2)	500	2500
Poisson's ratio (-)	0.2	0.2
E_1 (GPa)	8.5	32
E_2 (GPa)	0.35	32
G_{12} (GPa)	0.7	13.3
G_{23} (GPa)	0.05	13.3
G_{31} (GPa)	0.7	13.3
Structural damping, η (-)	0.06	0.02

The finite element program used is contained within the *GCity* program. For modelling plates, 4-noded quadrilateral shell elements are used with the ability to divide the plate into different layers, which was useful when modelling the CLT-plates. For beams and pillars, three dimensional beam elements were used.

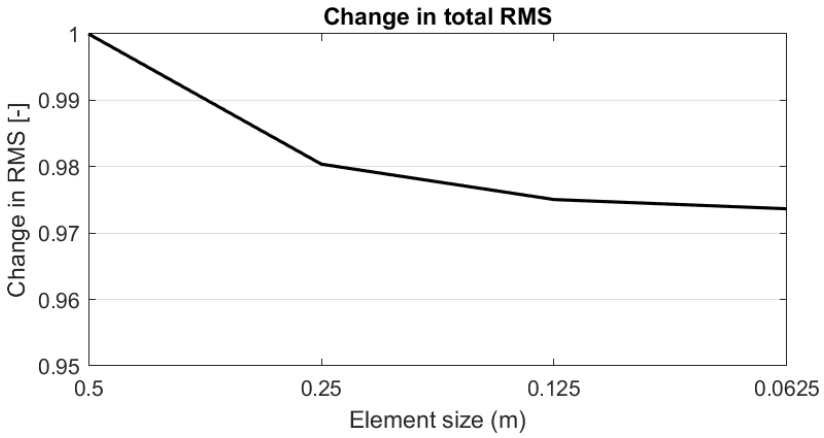

Figure 4.2: Result of the convergence study.

In order to determine an discretization for the finite element mesh, a convergence study was conducted. The results of the convergence study can be seen in Figure 4.2. As there is no significant difference of response beyond 0.25 m large elements and the computing time increased significantly with smaller elements, an element size of 0.25 m for both beam and shell elements were used.

The building is placed with the long side facing the excitation. The distance between the center of the building and the load point, or center of the railway, is 30 m in the standard case.

4.2 Ground model

In order to investigate the effect of the grounds dynamical behavior on the building vibration levels, three different sets of ground parameters were used in this dissertation. The first set is named the standard case, where the soil's large response frequencies did not match any eigenfrequencies of the standard cases of the building model. Furthermore, the model should represent plausible soil conditions. As such, the soil consists of a 6 m deep layer of a clay-like material followed by a semi-infinite layer of bedrock.

The two other ground models used were designed such as their large frequency responses matched one of the eigenfrequencies of the standard building cases for the wooden building and the concrete building, respectively. This was accomplished by altering the soil density and Young's modulus, while keeping the layer depth and bedrock parameters unchanged. These models were named "Matching wood" and "Matching concrete". A higher eigenmode to match was chosen for the concrete building in order to avoid overlap in the soil response. The free field response of the soil and the building's eigenmodes, respectively, can be found in Appendix A.

The properties of the soil cases and the bedrock can be found in Table 4.3.

Table 4.3: Ground Properties for all cases.

Case	Soil: Standard Case	Soil: Matching wood	Soil: Matching concrete	Bedrock
Depth (m)	0 - 6	0 - 6	0 - 6	6 - ∞
Density (kg/m^3)	1800	1500	1700	2500
Youngs module (MPa)	800	16	300	10 000
Poisson's ratio (-)	0.48	0.48	0.48	0.48
Loss factor (-)	0.10	0.10	0.10	0.04

4.3 Vehicle and track model

For the mixed FOR model, a vehicle and track model had to be defined. Using the *SubGCity* program, the vehicle and tracks could be defined through several parameters. A single vehicle was modeled as a 10-DOF multibody system as per Chapter 3.5.2. The properties of this vehicle are shown in Table 4.4. The track properties can be seen in Table 4.5. The values are taken from Bucinskas et al. [19].

Table 4.4: Vehicle properties.

Mass of car body (kg)	40 000
Mass of bogie (kg)	5 000
Mass of wheel set (kg)	1800
Car body pitch moment of inertia (kg^2)	$2.0 \cdot 10^6$
Primary suspension stiffness (N/m)	$2.4 \cdot 10^6$
Secondary suspension stiffness (N/m)	$6.0 \cdot 10^5$
Primary suspension damping (N $\cdot$ s/m)	30 000
Secondary suspension damping (N $\cdot$ s/m)	20 000
Distance between bogies' centers (m)	19.0
Distance between bogie's wheels sets (m)	2.7
Herztian constant G_H (-)	$5.4 \cdot 10^{-8}$

The rail unevenness was modeled through the use of a PSD-function from a German track spectrum, described by [21]. The track quality coefficient A_p was equal to $0.59233 \cdot 10^{-6}$ which corresponds to a medium quality track [19]. The train loading had excitation frequencies between 0 - 250 Hz, with 251 discrete frequencies.

4.4 Parameters

This section explains what parameters were tested for each parameter study, and their values. Most parameters were determined by estimating what changes to the building would logically have a impact on the dynamic behavior of the building, and some

Table 4.5: Track properties.

Rail mass per unit length (kg/m)	60.0
Rail bending stiffness (N/m^2)	$6.4 \cdot 10^6$
Rail loss factor (-)	0.01
Rail pad stiffness (N/m)	$5.0 \cdot 10^8$
Rail pad loss factor (-)	0.1
Sleeper mass per sleeper (kg)	542.0
Ballast vertical stiffness ($N \cdot s/m$)	$4.64 \cdot 10^9$
Ballast mass per unit length (kg/m)	1740
Ballast loss factor (-)	0.04
Track width (m)	3.2

were found to warrant further study during the testing phase and were included in the study. For the parameter study of a stationary load, the parameters tested are found in Table 4.6. The number of floors is defined as the number of different floor plates present, including the roof. The cross section parameter values were selected based on dimensions commonly found in the building industry.

Table 4.6: Parameters tested for a stationary load, with standard cases in bold.

Parameter	Wood Values	Concrete values	Unit
Soil type	**Standard** / Match. wood / Match. concrete		-
Number of floors	2 / **3** / 4 / 5 /6		-
Long side length	8 / 10 / **12** / 14 / 16		m
Short side length	4 /6 / **8** /10 / 12		m
Distance to load	10 / 20 / **30** / 40		m
Beam dimensions	90x315 / **115x360** / 140x405	150x300 / **200x400** / 250x500	mm
Pillar dimensions	110x110 / **160x160** / 210x210	150x150 / **200x200** / 250x250	mm
Structural damping	0.02 / 0.04 / **0.06** / 0.08 / 0.1	**0.02** / 0.04 / 0.06 / 0.08 / 0.1	-
Layers of CLT	5 / 6 / **7** / 8 / 9	-	-
Thickness of CLT layers	20 / 30 / **40** / 50 / 60	-	mm
Thickness of concrete slabs	-	150 / **200** / 250 / 300	mm

For the parameter study of the moving train load, the most impactful parameters were selected for an additional parameter study. Moreover, the speed of the train was also studied. The parameters and their values are found in Table 4.7.

Table 4.7: Parameters for the moving train load, with standard cases in bold.

Parameter	Wood Values	Concrete values	Unit
Distance to track	10 / 20 / **30**		m
Train speed	60 / 90 / **120**		km/h
Soil type	**Standard** / Match. wood / Match. concrete		-
Pillar dimensions	110x110 / **160x160** / 210x210	150x150 / **200x200** / 250x250	mm
Structural damping	0.02 / 0.04 / **0.06** / 0.08 / 0.1	**0.02** / 0.04 / 0.06 / 0.08 / 0.1	-

4.5 Evaluation of results

To evaluate the vibrations in the building and enable comparisons between both varying parameters and materials, four different evaluation measures where used. The stationary load case and the moving load case were evaluated with the same methods. Firstly, the steady state velocity amplitudes, or the equivalent velocity amplitude in the frequency domain for the *SubGCity* program, over 159 discrete frequencies between 1 Hz and 80 Hz were evaluated at 27 different points spread across one half of the floor as seen in Figure 4.3. Then an RMS-value representing all points was calculated for each evaluated frequency, using Equation 3.11. By plotting this velocity, the overall response of the building for each frequency could be examined.

The second evaluation measure was to calculate the overall RMS-value by once again using Equation 3.11 and evaluating the first measure over all discrete frequencies. A single value representing the vibration across the building was then acquired, which could be used to make simple comparisons without examining the frequency dependent response.

The third measure was to normalize the second measure against the maximum value for each building type and parameter study to be able to examine the change in percent for a given parameter study. This measure was used to gauge the relative impact a change in a certain parameter could have. It was calculated as

$$V_{Norm,i} = \frac{v_{RMS,i}}{max(\mathbf{v}_{RMS})} \tag{4.1}$$

where $V_{Norm,i}$ is the normalized RMS of velocity for one case i, $v_{RMS,i}$ is the velocity amplitude of the building for one case, and $\mathbf{v}_{RMS}$ is a vector containing the velocity amplitude for all cases.

The fourth and final measure was to calculate a building amplification factor that shows how the relation between the building velocity amplitudes from measure one and the ground velocity amplitudes according to

$$\mathbf{A} = \frac{\mathbf{v}_{RMS}}{\mathbf{v}_{ground}}. \tag{4.2}$$

Here, $\mathbf{A}$ is a vector containing the building amplification factors and $\mathbf{v}_{ground}$ is a vector containing the velocity amplitudes for a surface point in the center of the building.

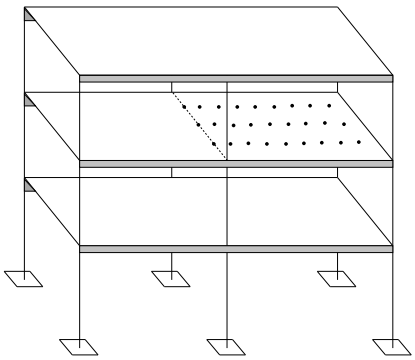

Figure 4.3: The distribution of measurement points over the building.

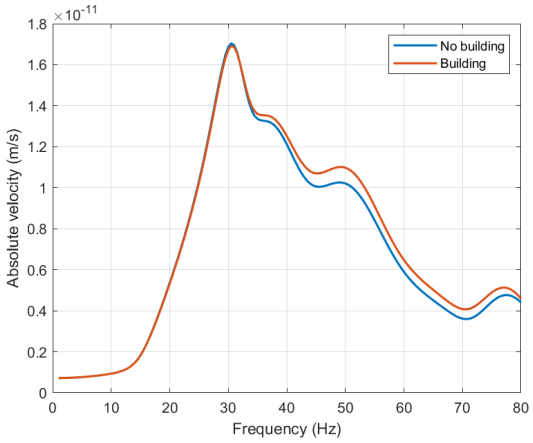

Figure 4.4: Difference between the free field response of the ground surface and the response with a building present using a stationary load.

The division is conducted as element-wise division for each discrete frequency. As the presence of the building may have an impact on the soil response $\mathbf{v}_{ground}$ a comparative study for a point with a building present versus the free field response was conducted, see Figure 4.4. The percentage difference in RMS of absolute velocity was 3.2%, and the response diverges slightly around 30 Hz and above. As the difference is small, the choice was made to use the response with the building present as this reduced calculation time.

The relations between all measures can be seen as a flowchart in Figure 4.5.

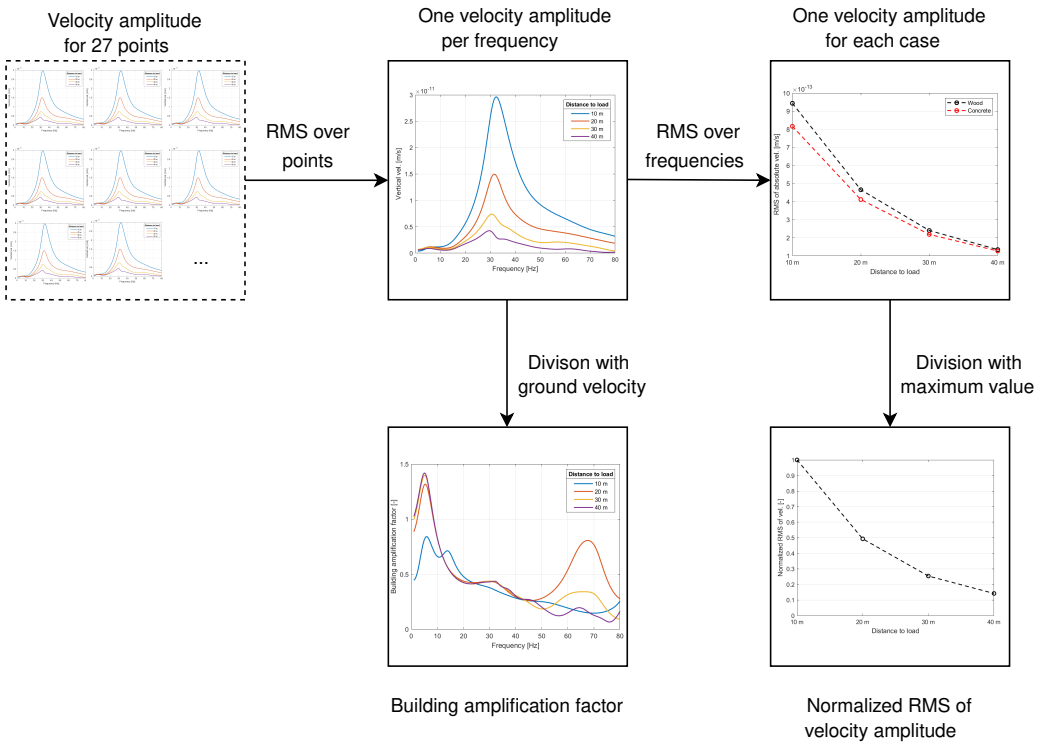

Figure 4.5: Flowchart of the relations between the different evaluation measures. Arrows represent calculations made.

5 Parameter studies

In this chapter the results of the parameter studies are presented. The results for the wooden building and concrete building are presented, as well as a comparison between the two building types.

5.1 Parameter study for stationary load

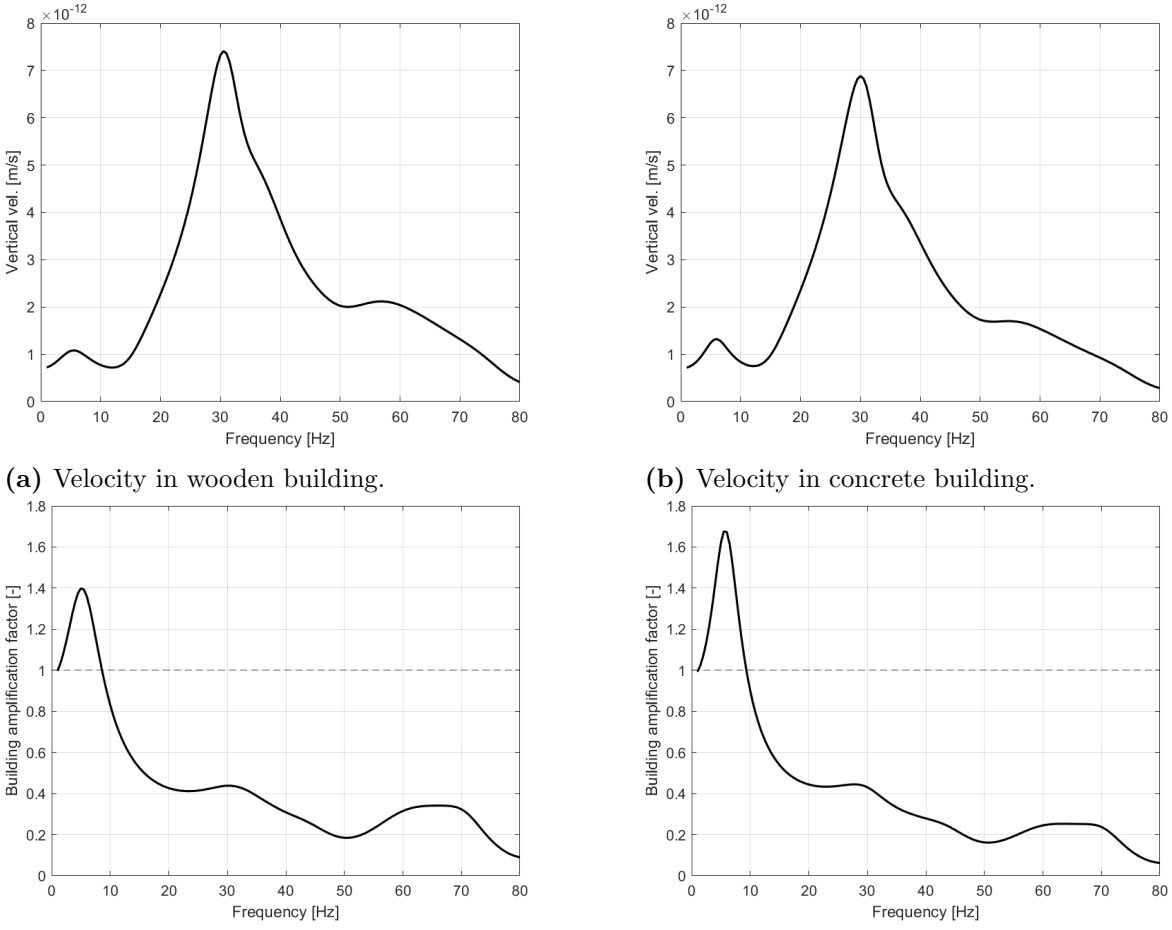

(a) Velocity in wooden building.

(b) Velocity in concrete building.

(c) The building amplification factor in the wooden building.

(d) The building amplification factor in the concrete building.

Figure 5.1: Results for the standard buildings.

A parameter study for a stationary oscillating load was conducted and the results of that study is found in this Section. A load with an amplitude of 1 N was applied on the ground surface, on a rigid squared surface with a side length of 1.1 m at the load point. The parameter studies on varying CLT layer heights, number of CLT layers and concrete plate thickness only concerned the respective building types and

no comparison was made for these cases. These are presented last. The results for the standard cases are presented in Figure 5.1.

5.1.1 Soil type

A defining feature of the study of soil type was the large peak in velocity amplitude for the Matching wood soil type as seen in Figures 5.2a and 5.2b. This shows that the soil conditions have a large impact on the measured vibration levels, and that for a soil with a low Young's modulus like the Matching wood type, the frequencies with the largest response are in the 1-15 Hz range. For the other two soil types, the frequencies with high response are higher and spread over a larger frequency range, between 10-50 Hz for the Matching Concrete type and 15-80 Hz for the Standard type as seen in Figure 5.3. The large impact of the soil type on overall vibration levels can also be seen in Figures 5.2c and 5.2d.

As seen in Figures 5.2e and 5.2f all three soil types induce a higher amplification of the vibrations in the low frequency range in the concrete building as opposed to the wooden building. This is despite the fact that the Matching wood and Matching concrete soil types were designed to cause a large response frequency in the ground motion at the building types respective natural frequencies, and in turn induce eigenmodes which would cause additional vibrations. While eigenmodes seem to have been induced in both buildings in the 1-12 Hz range, there is no definitive correlation between the "matching" soil types and their respective building material. It is also notable that both buildings seem to have a large amplification factor at roughly 72 Hz for the Matching concrete soil type, that is not present for the other soil types. It is not concluded why this amplification occurs here. A cause could be that the soil vibrations coincide with a higher natural frequency in both building types at this frequency, but this has not been investigated.

When comparing the two building types to each other in Figure 5.4 it was noted that the vibration levels in the concrete building was higher for the Matching wood soil type, but lower for the two other soil types. This shows that it is not only the building type that affects the vibration levels, but rather the combination of soil and building. For the studied standard building it means that for a very soft soil such as the Matching wood type, the better material choice is wood, while for the more stiff soil types the better material choice is concrete.

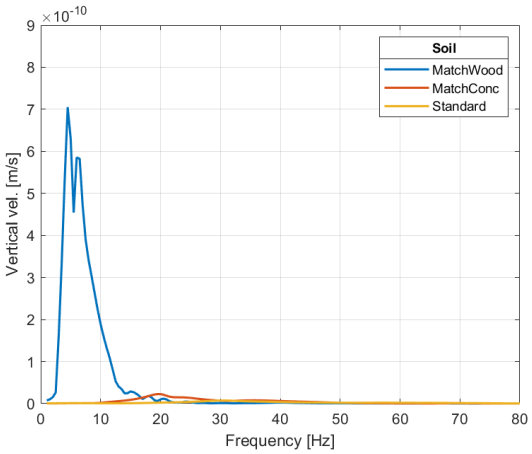

(a) Velocity in wooden building.

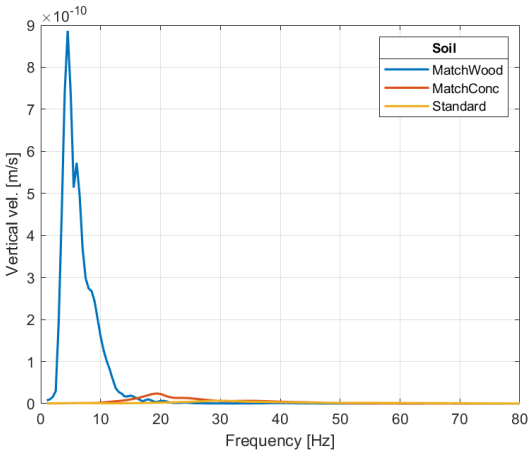

(b) Velocity in concrete building.

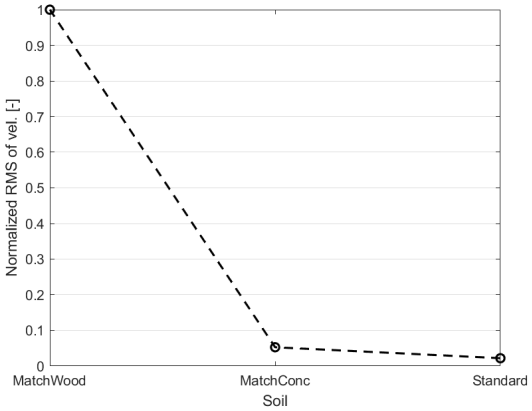

(c) Change of RMS in wooden building.

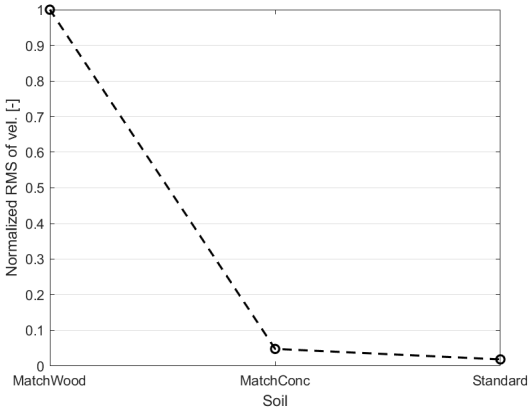

(d) Change of RMS in concrete building.

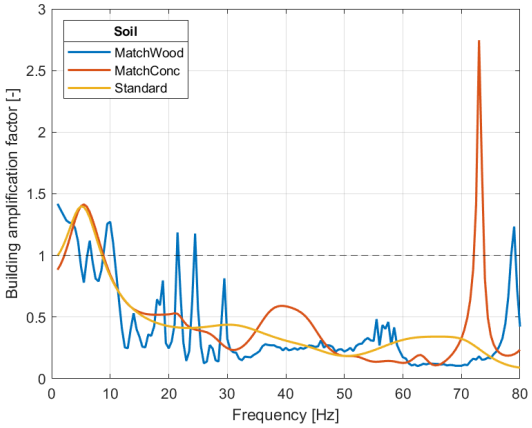

(e) Building amplification in wooden building.

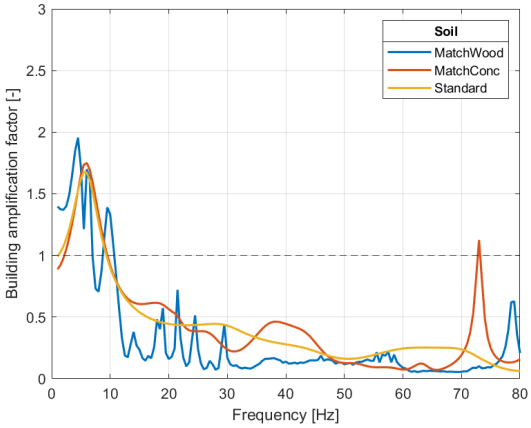

(f) Building amplification in concrete building

Figure 5.2: Results of the soil type parameter study.

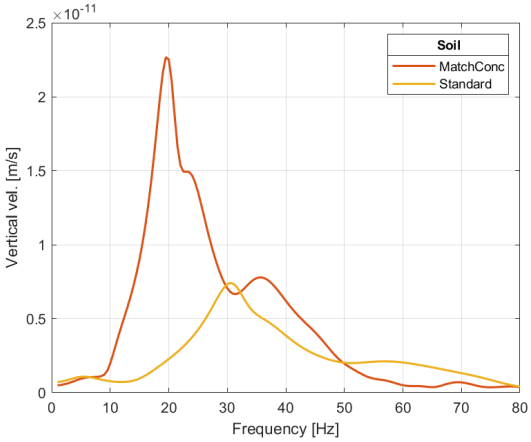

(a) Velocity in wooden building, upscaled version of Figure 5.2a.

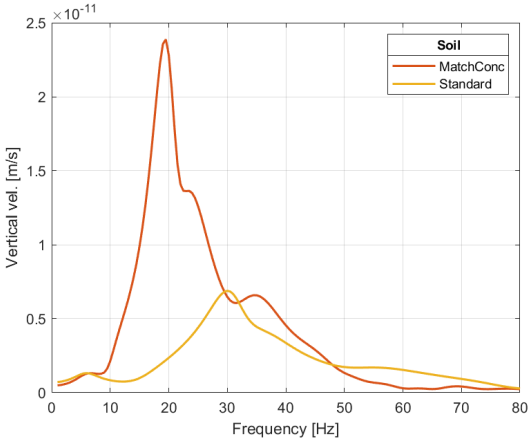

(b) Velocity in concrete building, upscaled version of Figure 5.2b.

Figure 5.3: Upscaled plots of the absolute velocities for the Standard and Matching concrete soil types.

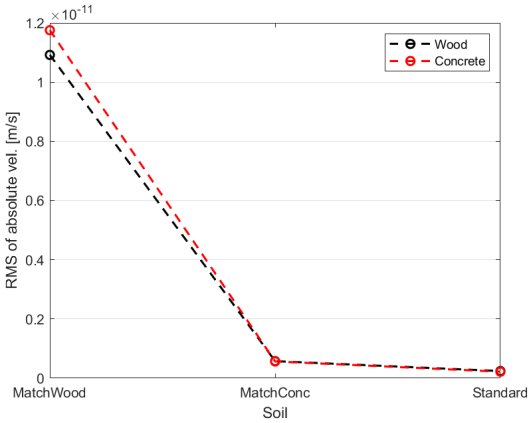

(a) Comparison of RMS of velocity.

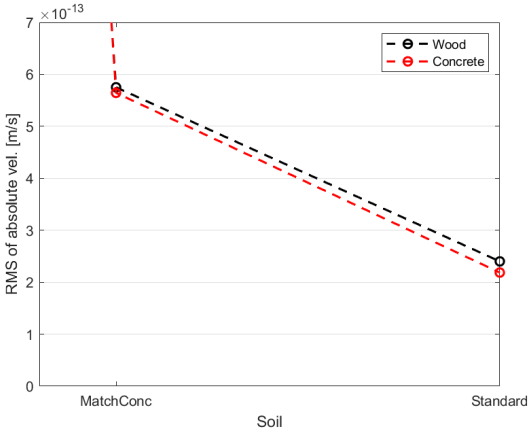

(b) Upscaled comparison.

Figure 5.4: Comparison of RMS of velocity. For all soil types and upscaled for clarity.

5.1.2 Number of floors

When examining the effect that changing the number of floors and thus the building height have on the vibration levels there emerges a trend. As seen in Figures 5.5c and 5.5d a higher number of floors results in lower vibrations at the top floor plate. The change seems to be linear and applies for both building types. However, note that as the measuring points are always placed on the second highest slab.

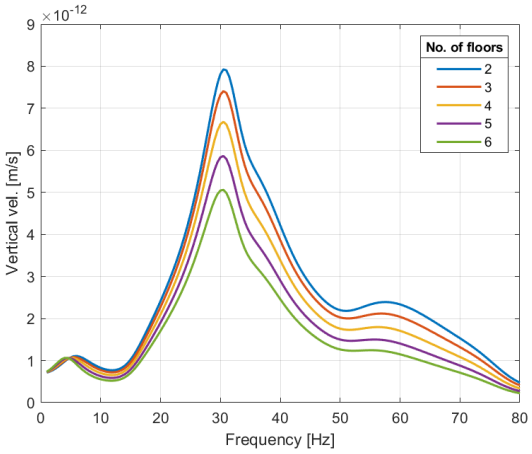

(a) Velocity in the wooden building.

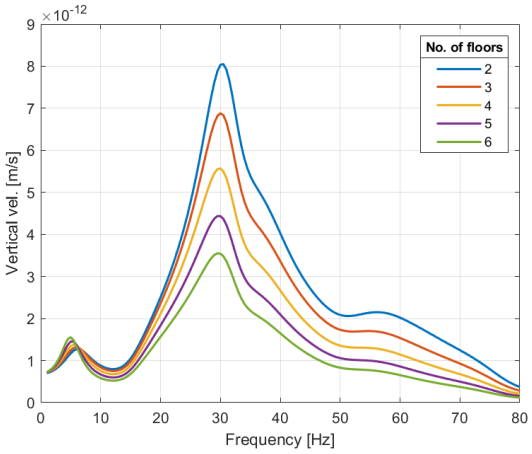

(b) Velocity in the concrete building.

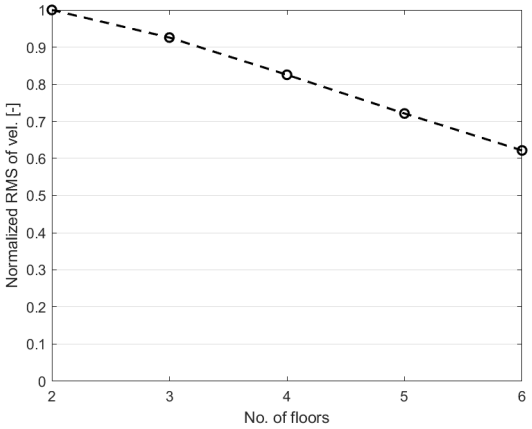

(c) Normalized RMS of velocity in the wooden building.

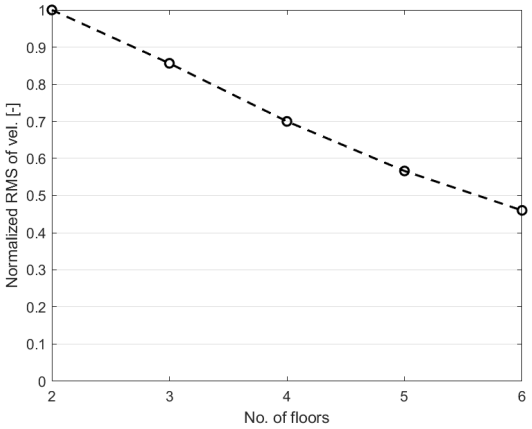

(d) Normalized RMS of velocity in the concrete building.

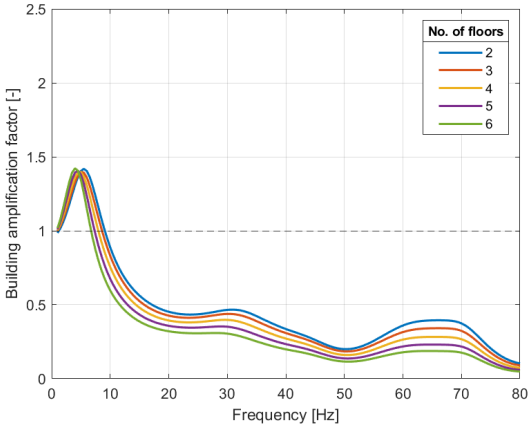

(e) Building amplification in wooden building.

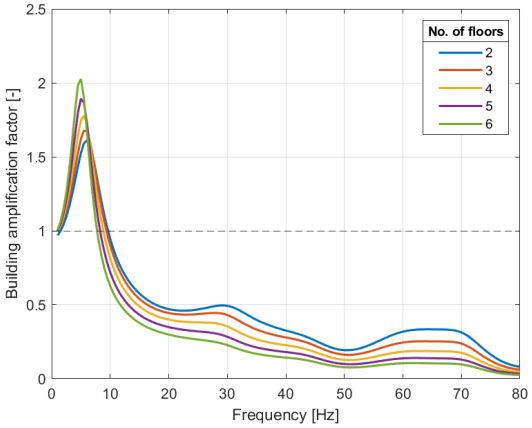

(f) Building amplification in the concrete building

Figure 5.5: Results of the parameter study of the number of floors.

As the distance from the building supports to the measuring points increases with more floor levels there exist more material which may dissipate energy through damping. With an increase in the number of floors there also comes an increase in the mass of the building and a different geometry. This may cause a shift in the natural frequencies of the building. Looking at Figures 5.5e and 5.5f the peak of the amplification factor in the low frequency range does shift lower as the number of floors increases. As the amplification factor is a indicator for when the building is resonating, this may show a shift in the natural frequencies of the building.

A notable result is the difference in amplification behavior of the two building types. For the wooden building, the shift in the building amplification's peak frequency in the 1-6 Hz range does not cause a difference in amplitude. In the concrete building, the shift also causes a higher amplitude as the peak frequency decreases with an increasing number of floors. The cause of this difference has not been investigated.

When comparing the two building types against each other in Figure 5.6, it can be noted that while the concrete building always has a lower RMS of velocity than the wooden building, the gap increases with a higher number of floors. This shows that as the building gets higher, the benefit of using concrete increases.

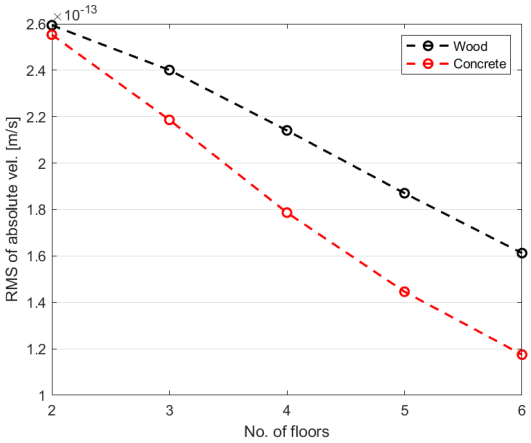

Figure 5.6: Comparison of RMS of velocity.

5.1.3 Length of the building

The length of the building has a significant impact on the vibration levels inside the building. As can be seen in Figures 5.7c and 5.7d there is a 38% reduction in RMS of velocity when doubling the length of the wooden building, and a 42% reduction in the concrete building. Furthermore, there seems to be a slight shift to a lower frequency of the peak building amplification in Figures 5.7e and 5.7f. This change in frequency of the peak coincides with a increase in amplification amplitude as the peak frequency decreases with a longer building length. This behavior is limited to the 1-8 Hz range, and at higher frequencies a longer building results in lower amplification.

As the building gets larger its mass increases, which may cause a reduction in vibration levels as more inertia has to be moved. Another factor may be the increased distance between the center of the floor slabs to the pillars. As it is the pillars which propagate

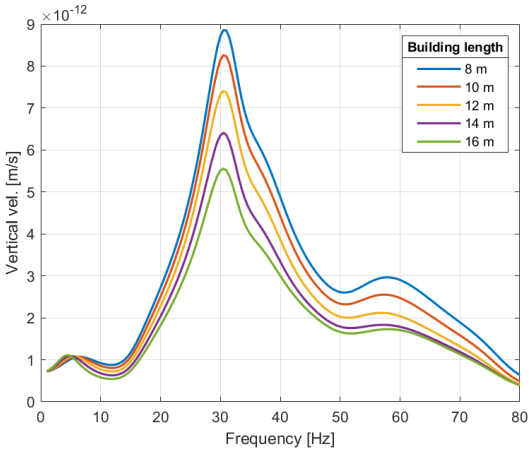

(a) Velocity in the wooden building.

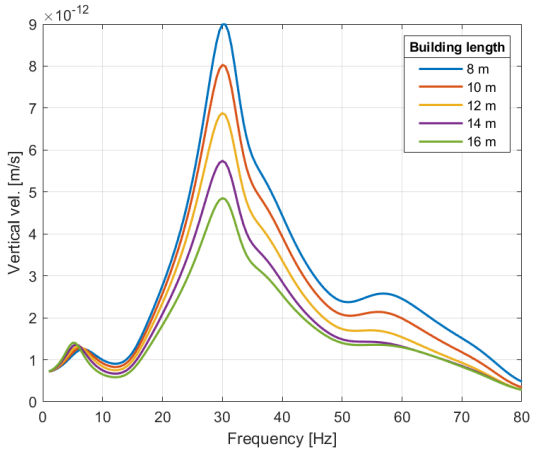

(b) Velocity in the concrete building.

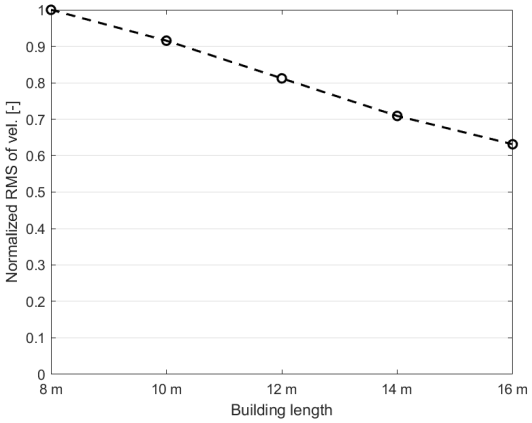

(c) Normalized RMS of velocity in the wooden building.

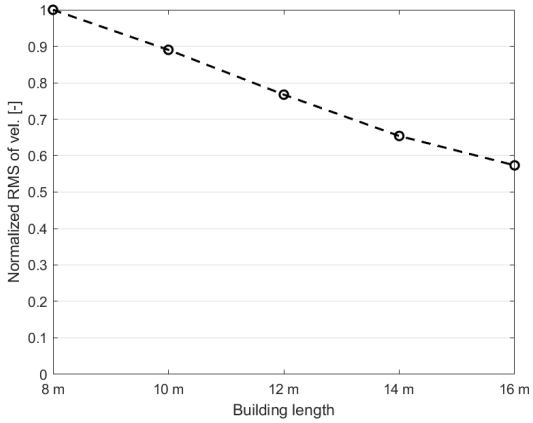

(d) Normalized RMS of velocity in the concrete building.

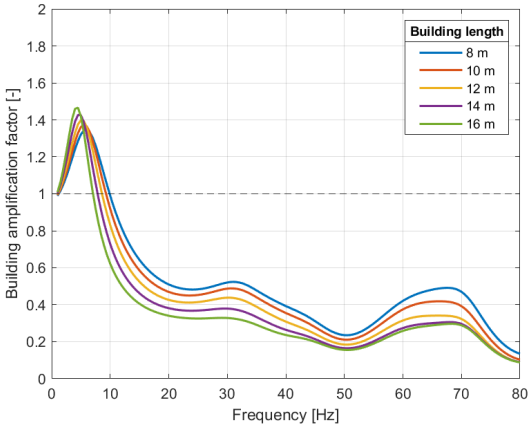

(e) Building amplification in wooden building.

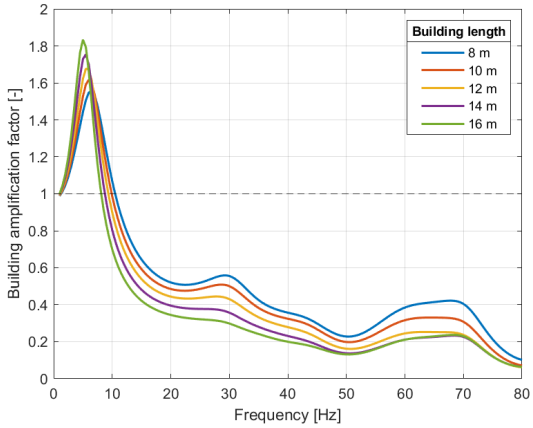

(f) Building amplification in the concrete building

Figure 5.7: Results of the parameter study of the building length.

the vibrations into the beams and slabs, the vibrations must move more material before reaching the center of the building, which may lead to energy losses in geometric damping in the ground and material damping.

A comparison of the two building types in Figure 5.8 reveals that the impact of the length on RMS of velocity is similar for both material choices. There seems to be

a slight increase in difference between the wooden and concrete buildings as length increases, with the wooden building always having the highest vibration levels.

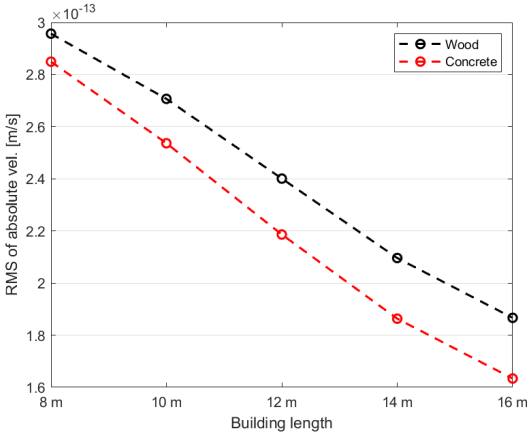

Figure 5.8: Comparison of RMS of velocity.

5.1.4 Width of the building

The effect of changing the width of the building has some similarities with changing the length. A wider building results in lower vibration levels, as seen in Figures 5.9c and 5.9d. The impact of mass may be somewhat similar. However when changing the width, the behavior is not as linear as when changing the length. Another differing behavior can be seen in Figures 5.9e and 5.9f.

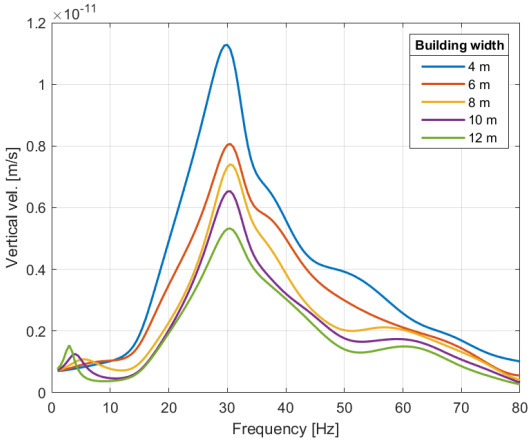

(a) Velocity in the wooden building.

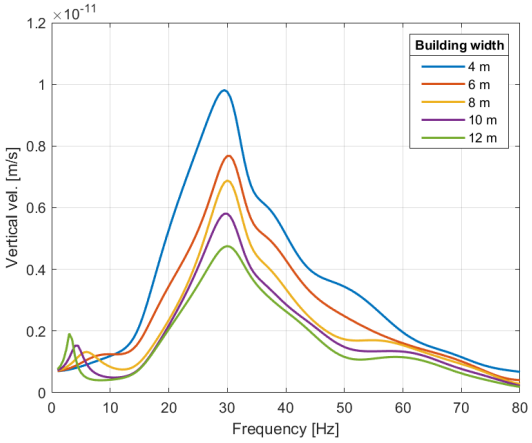

(b) Velocity in the concrete building.

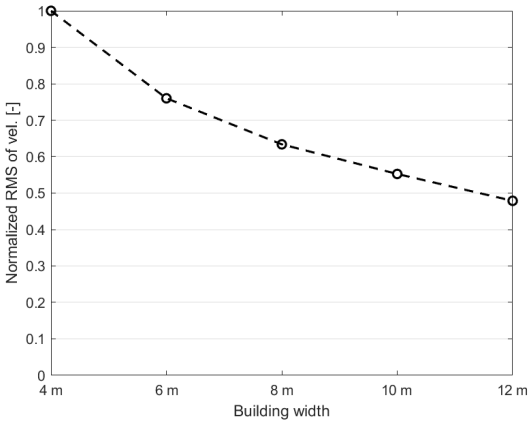

(c) Normalized RMS of velocity in the wooden building.

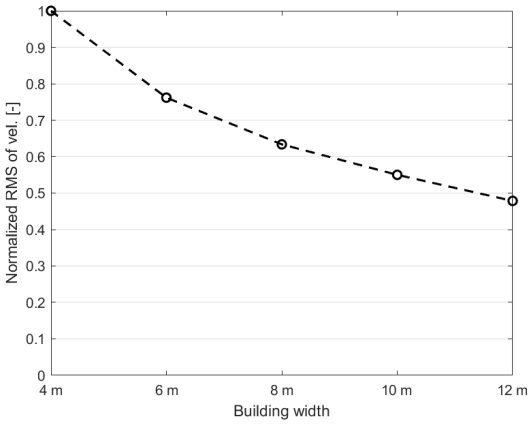

(d) Normalized RMS of velocity in the concrete building.

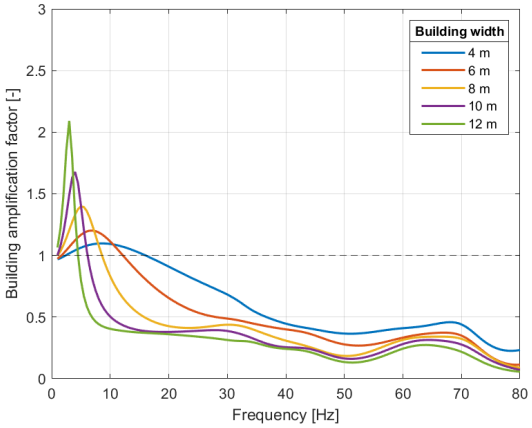

(e) Building amplification in wooden building.

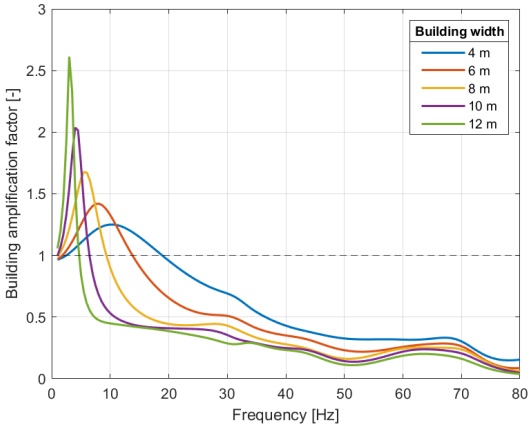

(f) Building amplification in the concrete building

Figure 5.9: Results of the parameter study of the building width.

Here it can be noted that the peak amplification changes dramatically depending on width, with wide buildings having a high and early peak while shorter widths results in low amplitudes but spread over a larger frequency band. A change in natural frequencies of the building is evident when the width changes. As this is the span direction of the floor plates, a longer span will generally result in lower natural frequencies for the bending modes of the plates. This explains the frequency of the peaks in the amplification factors, but not the width of the peaks.

This behavior may be caused by the placement of the pillars in relation to the load point. Increasing the width of the building moves the front pillars closer to the load point, while the back pillars are moved further away. This results in higher vibration transmission in the front pillars and lower transmission in the back pillars. Moreover, the change in distance between the front and back pillars means that the building may interact with the wave crests in the ground differently, e.g. the front pillars cresting a wave while the back pillars are in a trough. Dependent on if the wave propagation from the pillars to the plates are constructively on destructively interfering the measured vibration levels may increase or decrease, respectively. This may also impact the triggering of eigenmodes.

Comparing the two building types in Figure 5.10 shows that the effect of changing the width of the building is very similar for both types, with the shapes of the curves being near identical. As the effect of the width is the same, the wooden building always has higher vibration levels compared to the concrete building for the studied widths.

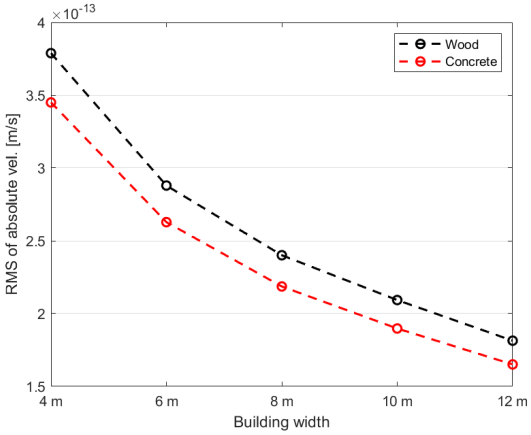

Figure 5.10: Comparison of RMS of velocity.

5.1.5 Distance to load

The distance to the load has a large impact on the measured vibration levels. The change in vibration levels due to varying the distance is not linear however, and examining Figures 5.11c and 5.11d it can be noted that the decay is seemingly exponential and the RMS decrease from 10 meters to 40 meters is around 85% for both buildings. By examining Figures 5.11e and 5.11f it can be seen that the building amplification differs substantially with distance. When the distance is 10 meters the impact from bending modes being excited is small, with the building vertical velocity never

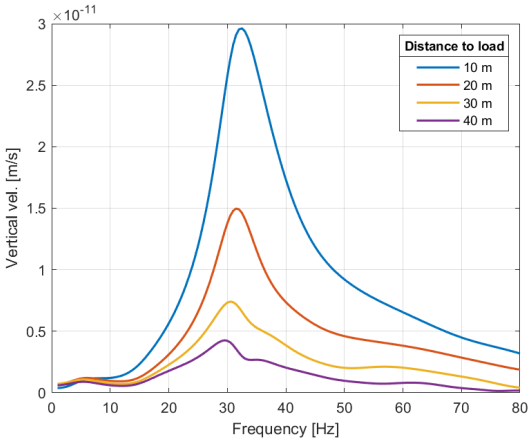

(a) Velocity in the wooden building.

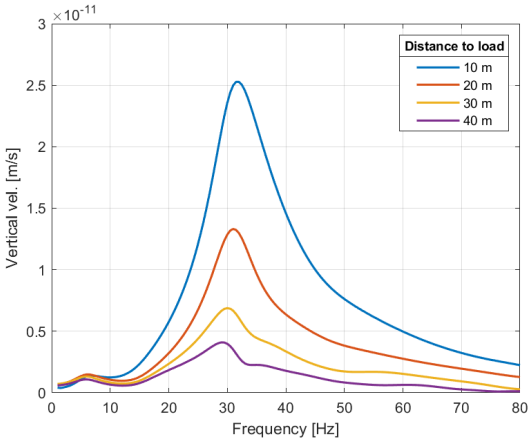

(b) Velocity in the concrete building.

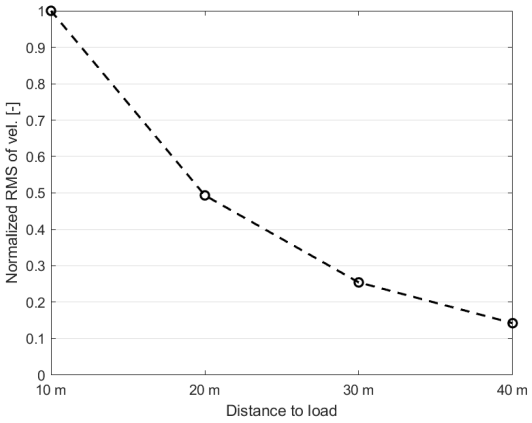

(c) Normalized RMS of velocity in the wooden building.

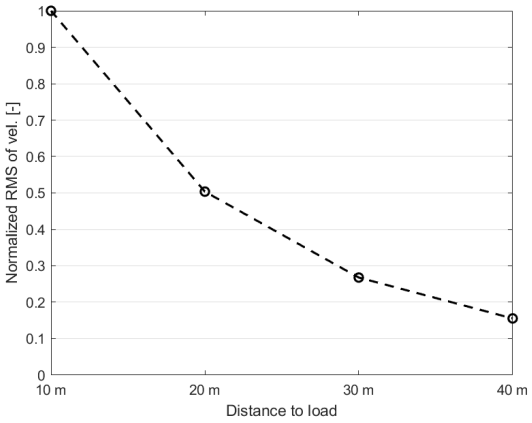

(d) Normalized RMS of velocity in the concrete building.

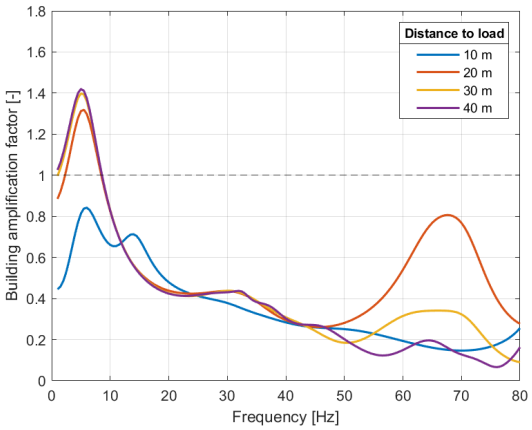

(e) Building amplification in wooden building.

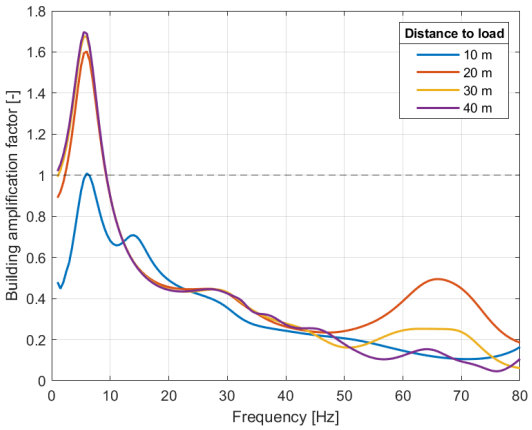

(f) Building amplification in the concrete building

Figure 5.11: Results of the parameter study of the distance to the load.

exceeding the ground motion for any frequency. Increasing the distance the impact from the bending modes becomes more pronounced in the low frequencies. Important to consider when examining these results is that the load distance is from the center of the building to the load, which means that when the distance to load is 10 meters the real distance from the foundations of the near pillars to the load is only 6 meters.

When comparing the two types of building in Figure 5.12 it can be noted that the

absolute difference between the building materials decreases with distance.

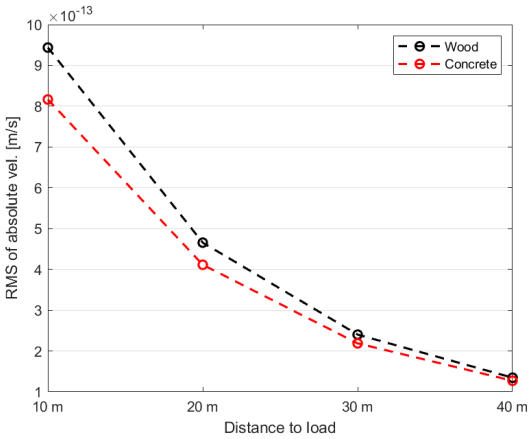

Figure 5.12: Comparison of RMS of velocity.

5.1.6 Cross section of beams

The effect of changing the beam cross section is one of the smallest for the examined parameters, as seen in Figures 5.14c and 5.14d. This result can be explained by the fact that the beams run perpendicular to the wave direction of the vibrations, and will not effect the vibration transmission from the pillars to the floor plates or the natural frequencies for the relevant bending modes.

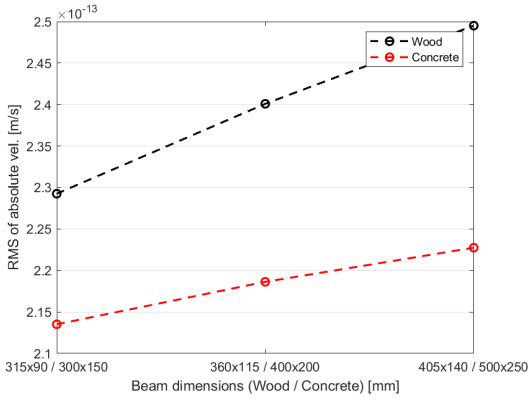

Figure 5.13: Comparison of RMS of velocity.

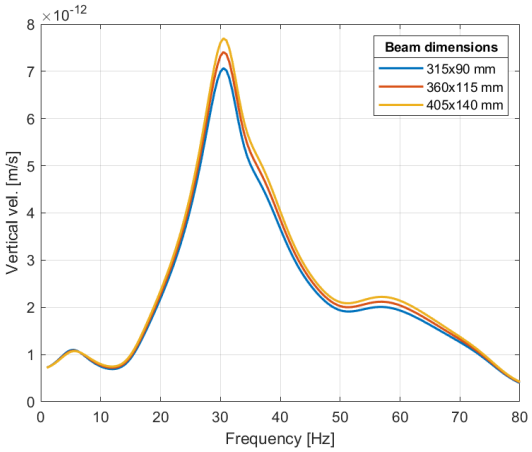

(a) Velocity in the wooden building.

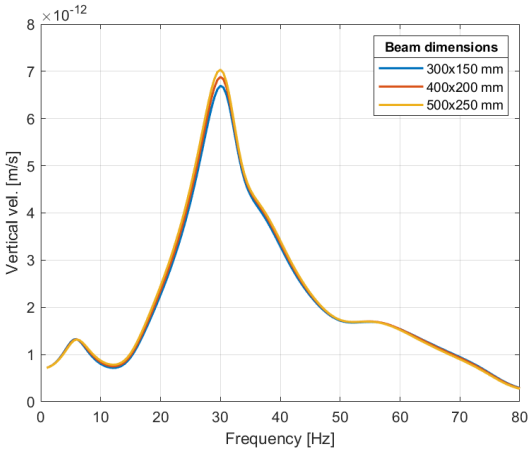

(b) Velocity in the concrete building.

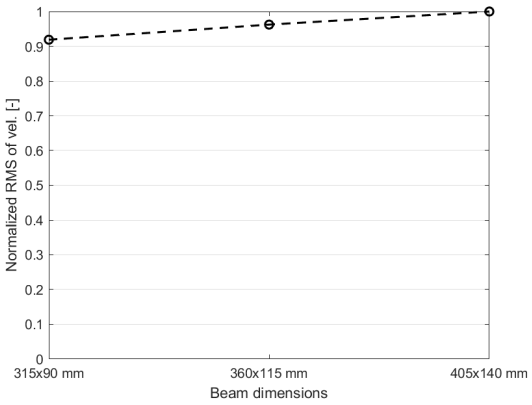

(c) Normalized RMS of velocity in the wooden building.

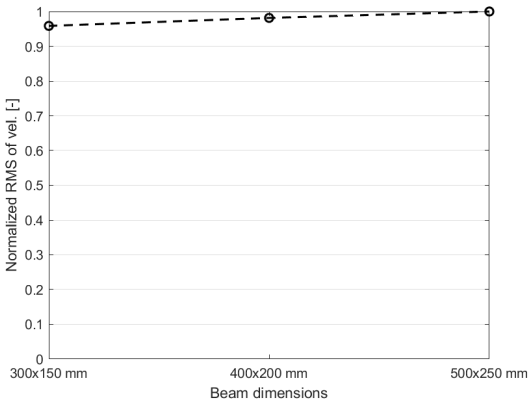

(d) Normalized RMS of velocity in the concrete building.

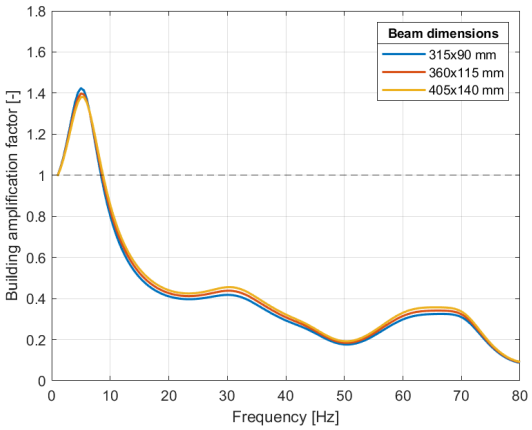

(e) Building amplification in wooden building.

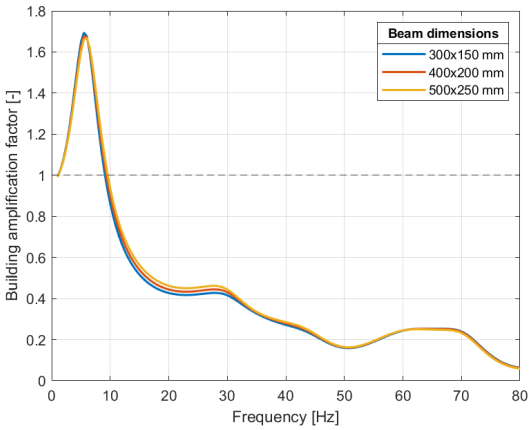

(f) Building amplification in the concrete building

Figure 5.14: Results of the parameter study of the beam cross-section.

5.1.7 Cross section of pillars

Examining the results of the study of pillar cross sections, it can be seen that the cross section has a large impact on vibration levels. In Figures 5.15c and 5.15d an approximately 3.6 times larger cross sectional area causes a 37% increase in RMS values for the wooden building, while a approximately 2.7 times large cross sectional area causes a 45% increase in RMS values for the concrete building. Why changing

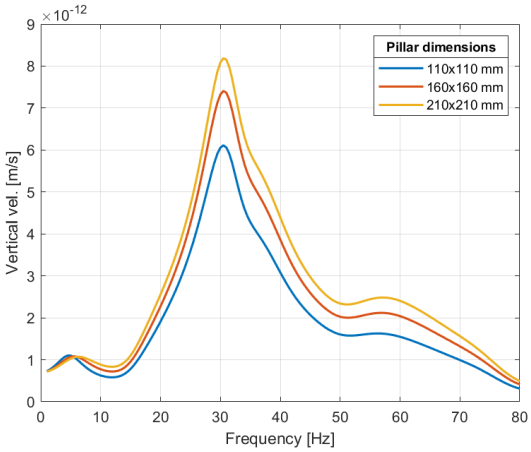

(a) Velocity in the wooden building.

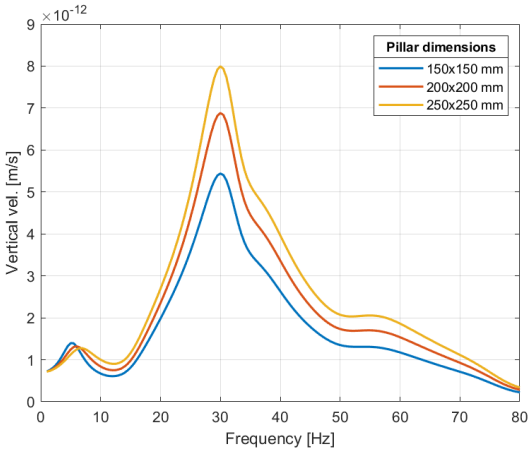

(b) Velocity in the concrete building.

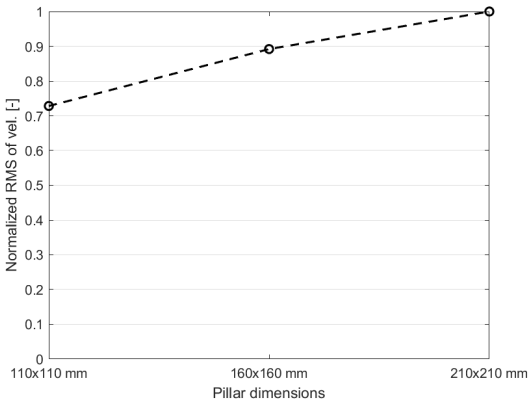

(c) Normalized RMS of velocity in the wooden building.

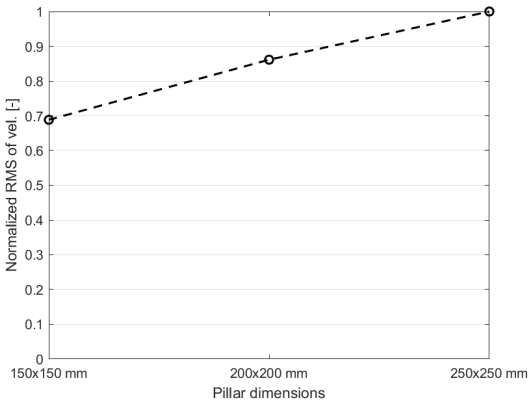

(d) Normalized RMS of velocity in the concrete building.

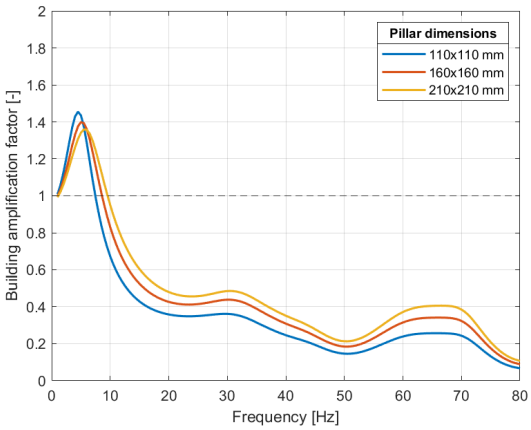

(e) Building amplification in wooden building.

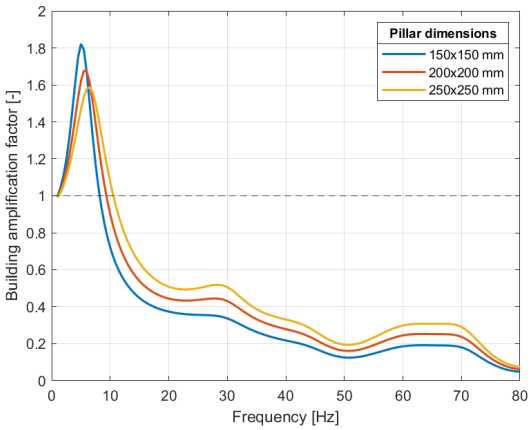

(f) Building amplification in the concrete building

Figure 5.15: Results of the parameter study of the pillar cross-section.

the pillar cross section has a large effect on measured vibrations is further discussed in Section 5.1.8. As seen in Figures 5.15e and 5.15f there seems to be a slight shift in the frequency of the peak building amplification factor as the dimensions increase, which indicates a shift in natural frequency of the building. Comparing the two building types in Figure 5.16 the effect of changing the cross section seems to be similar for both buildings.

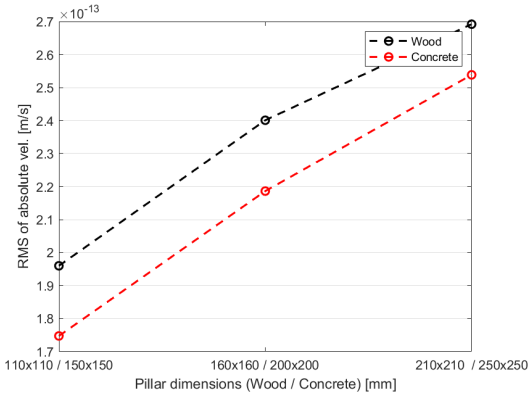

Figure 5.16: Comparison of RMS of velocity.

5.1.8 Damping

The effect of structural damping on the measured RMS can be seen in Figures 5.18c and 5.18d. As damping increases, so does the RMS value. This result is counterintuitive, as more energy losses in the material results in higher vibrations. Examining Figures 5.18a and 5.18b it can be found that for the velocity peak in the 1-8 Hz range, the behavior of higher damping resulting in lower vibration levels is present. At around 8 Hz, the behavior switches.

Studying Figures 5.18e and 5.18f, the same behavior can be seen. When the building amplification factor is above one and the building is resonating in its bending modes, the effect of the damping is as expected, but when the building no longer amplifies the soil vibrations the behavior reverses. This means that higher damping increases the transmission of vibrations from the soil to the building when the vibration response is driven by ground vibration, i.e., amplification factor below 1.

A plausible mechanism for this might be that as damping increases so does the dynamic stiffness of the pillars. With stiffer pillars, the transmission of vibrations into the floor plates increases as the pillars bend less. This may therefore also be applicable in Section 5.1.7 where the similar behavior of stiffer pillars resulting in higher vibration levels is observed, which supports the hypothesis.

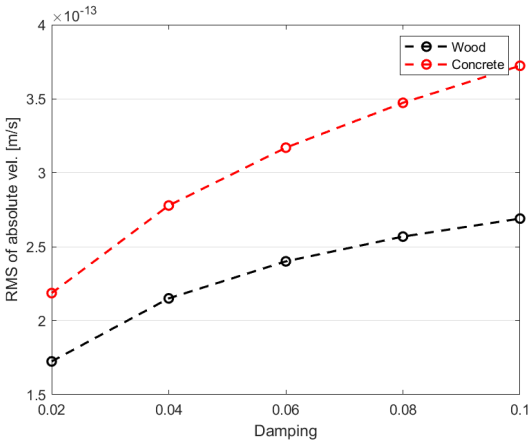

Figure 5.17: Comparison of RMS of velocity.

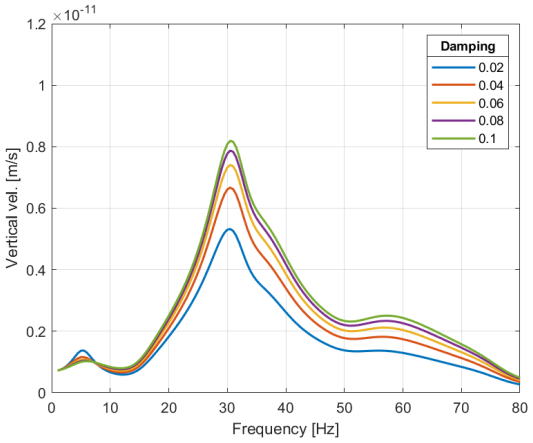

(a) Velocity in the wooden building.

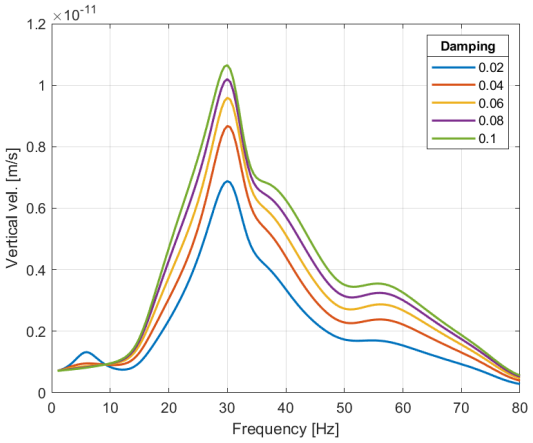

(b) Velocity in the concrete building.

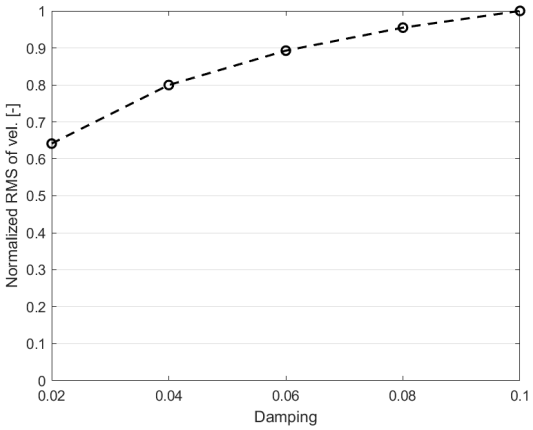

(c) Normalized RMS of velocity in the wooden building.

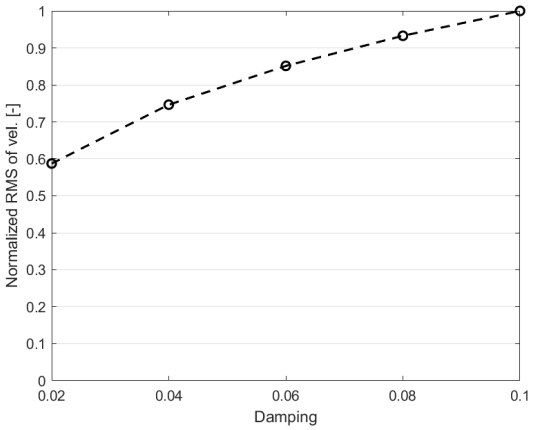

(d) Normalized RMS of velocity in the concrete building.

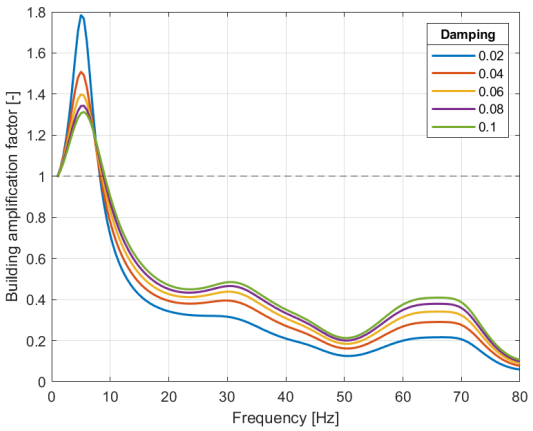

(e) Building amplification in wooden building.

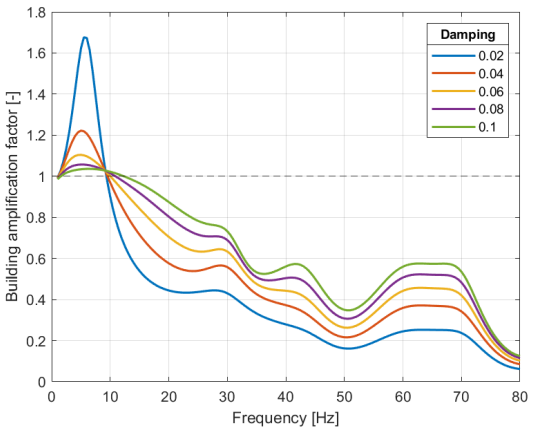

(f) Building amplification in the concrete building

Figure 5.18: Results of the parameter study of structural damping.

The comparison in Figure 5.17 shows that the effect is more pronounced for the concrete building than for the wooden building. The Figure also shows that for a wooden and concrete building with the same damping, the concrete performs worse. This means that it is plausible for a wooden building with low structural damping to outperform a similar concrete building with high structural damping.

5.1.9 Thickness of CLT floors

Number of CLT layers

The effect of the number of layers of CLT on the measured vibration levels is negligible as seen in Figure 5.19b, with a maximum decrease of RMS of 4% and no obvious trend. There is a slight change of natural frequency as seen in Figure 5.19c, with a thicker CLT plate resulting in a slightly higher peak amplification frequency.

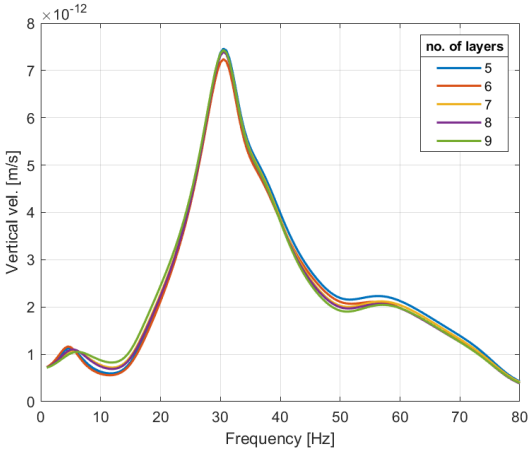

(a) Velocity in the wooden building.

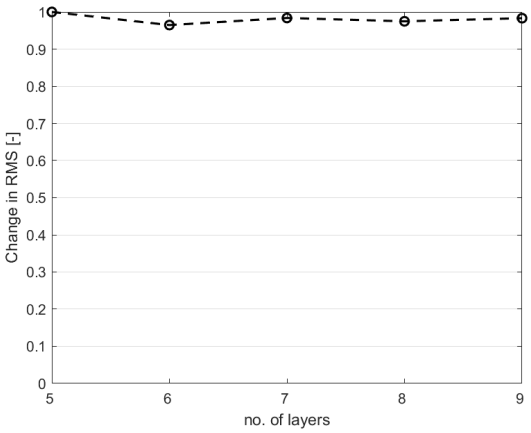

(b) Normalized RMS of velocity in the wooden building.

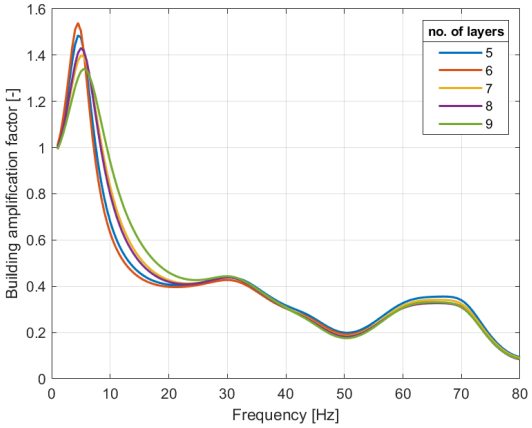

(c) Building amplification in the wooden building.

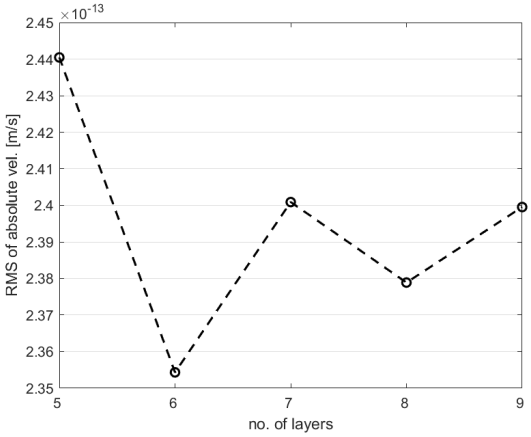

(d) RMS of absolute velocity in the wooden building.

Figure 5.19: Results of the parameter study of the number of CLT layers.

Thickness of CLT layers

The thickness of CLT layers has a similar effect on vibration levels as the changing the number of layers. As the thickness of the CLT plates increases, there is a small increase in natural frequency in Figure 5.20c but no significant change of RMS or trend in Figure 5.20b.

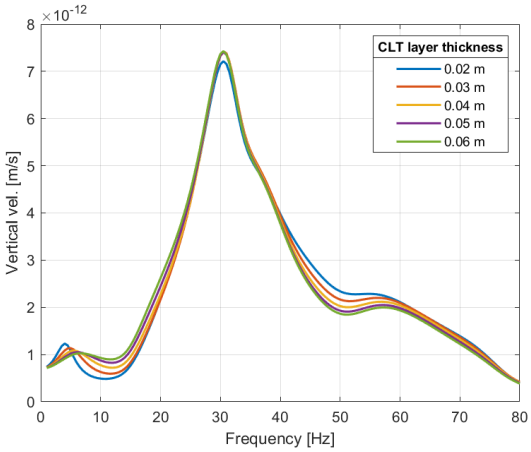

(a) Velocity in the wooden building.

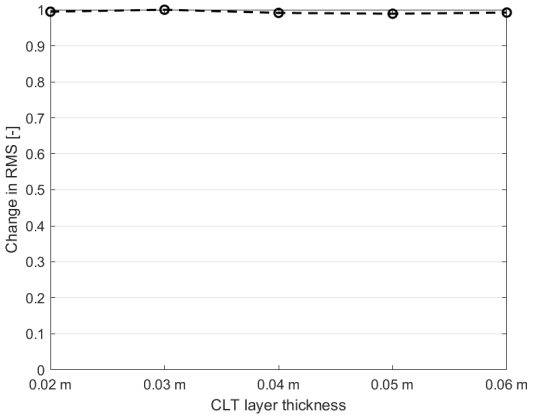

(b) Normalized RMS of velocity in the wooden building.

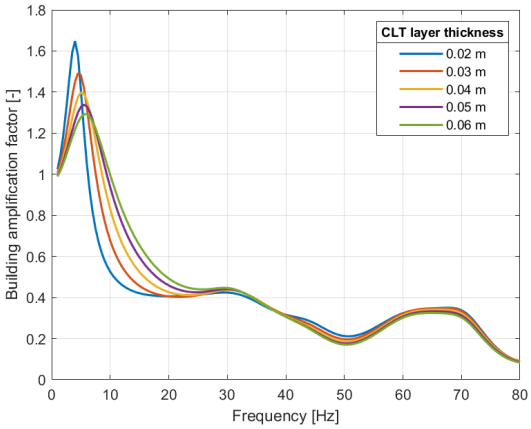

(c) Building amplification in the wooden building.

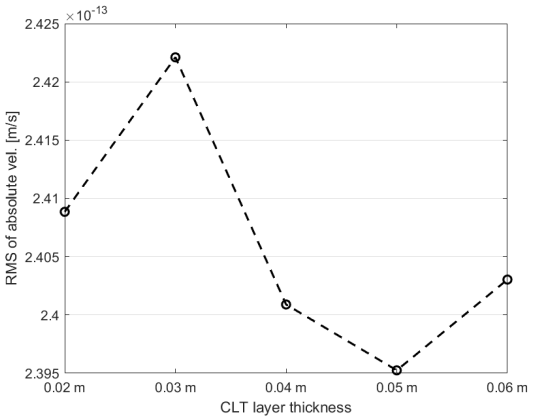

(d) RMS of absolute velocity in the wooden building.

Figure 5.20: Results of the parameter study of the thickness of CLT layers.

5.1.10 Thickness of concrete floor

Similar to when changing the thickness of the CLT plates in the wooden building, changing the concrete floor thickness results in a small change in vibration levels. In Figure 5.21b the increase in concrete thickness results in lower RMS velocities in the building, with a doubling of thickness resulting in a 8% decrease. While more than for the CLT plates, it is still a comparatively small decrease for the overall parameter study.

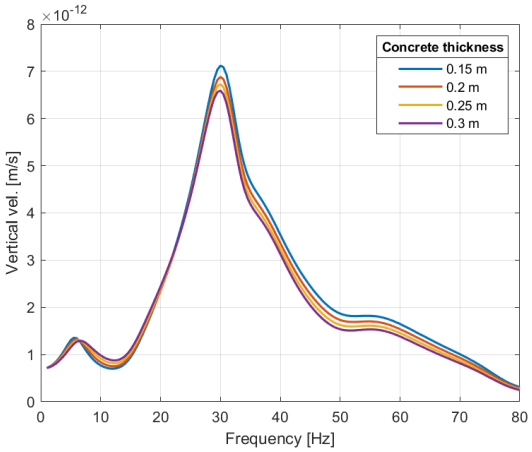

(a) Velocity in the concrete building.

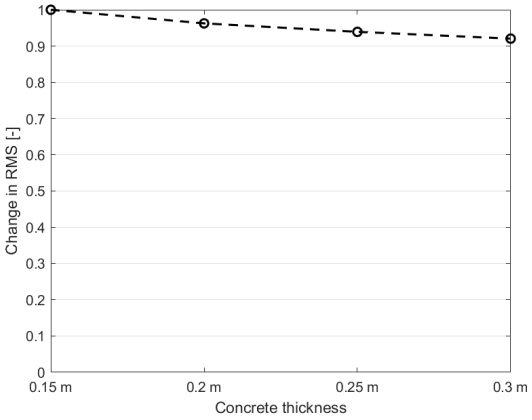

(b) Normalized RMS of velocity in the concrete building.

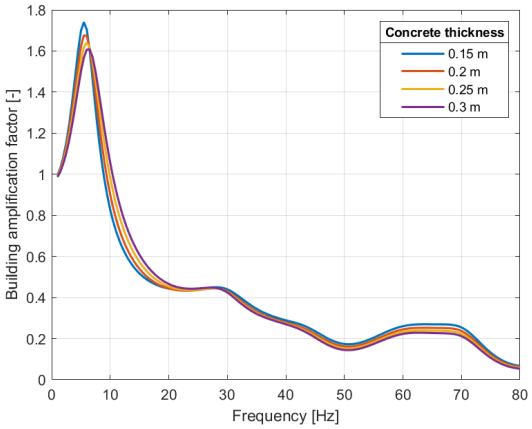

(c) Building amplification in the concrete building.

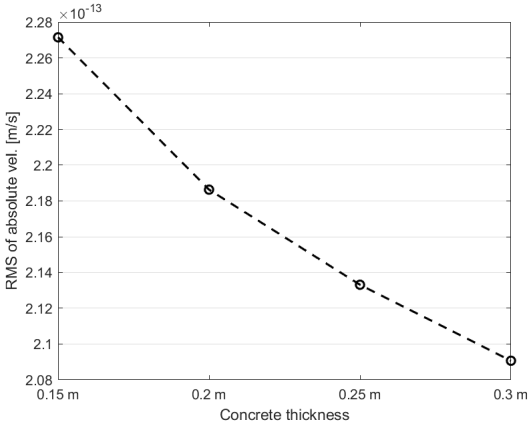

(d) RMS of absolute velocity in the concrete building.

Figure 5.21: Results of the parameter study of the thickness of concrete floors.

5.2 Study of moving train load

A limited parameter study with a more computationally heavy moving train load was conducted using the *SubGCity* program. The most significant parameters from the parameter study of the stationary load were selected. The parameters were: distance to load, cross section of pillars, damping and soil type. Of the selected parameters, damping and soil type are investigated for the wooden building solely.

5.2.1 Distance to track

The distance to the track seems to have a high impact on the measured vibrations. Examining Figures 5.22c and 5.22d the RMS value decrease when going from 10 to 30 meters is 77 % for the wooden building and 85 % for the concrete building. Studying Figures 5.22a and 5.22b the effect is highest in the 1-6 Hz range, and is then somewhat lower in the 8-25 Hz rage before increasing again for frequencies above 25 Hz. As seen in Figure 5.22e the amplification factor of the wooden building does not reach one at any point. This means that while resonance may occur, such as the peaks in

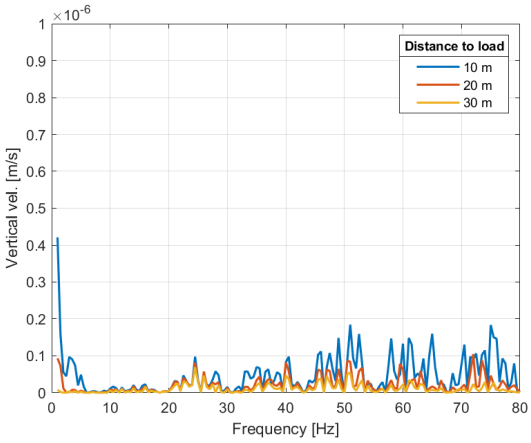

(a) Velocity in the wooden building.

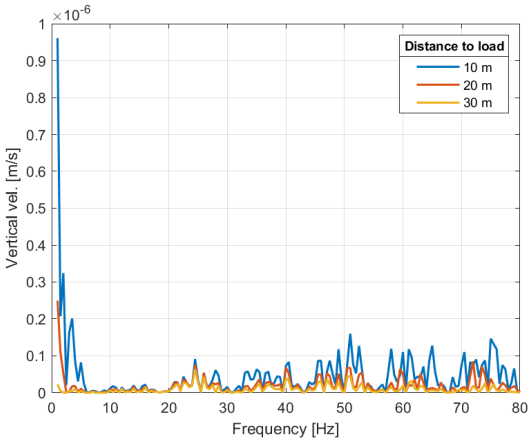

(b) Velocity in the concrete building.

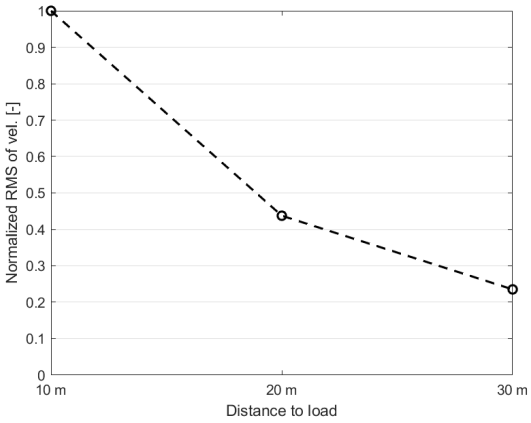

(c) Normalized RMS of velocity in the wooden building.

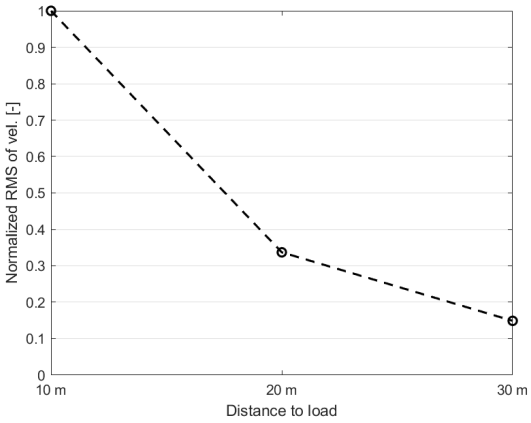

(d) Normalized RMS of velocity in the concrete building.

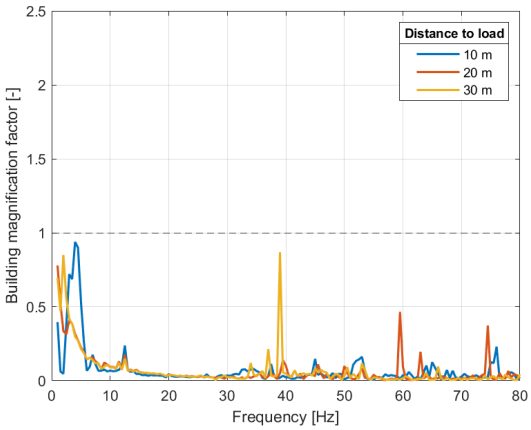

(e) Building amplification in the wooden building.

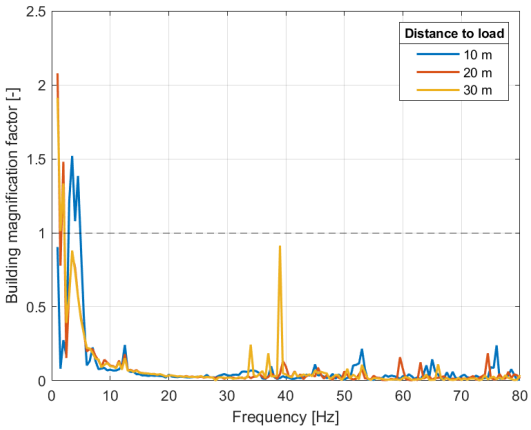

(f) Building amplification in the concrete building

Figure 5.22: Results of the parameter study of the distance to the track.

the low frequency range, this resonance does not cause the vibrations in the building to exceed the ground vibrations. In opposition, examining Figure 5.22f the concrete building seems to have a higher amplification factor indicating that the resonance in the low frequencies is more impactful than for the wooden building. Both building types also seem to have some amplification peaks at the higher frequencies, especially around 39 Hz.

Comparing the RMS of the velocity between the two types of building in Figure 5.23 it can be seen that the wooden building performs better at low distances from the railway, while the concrete building performs better at 30 meters distance. This is opposed to the findings in Section 5.1.5 where it found that the concrete performed better at short distances to the rail and the two building types performed more similarly as the distance increased. This indicates that the stationary parameter studies may have limitations in examining railway vibrations.

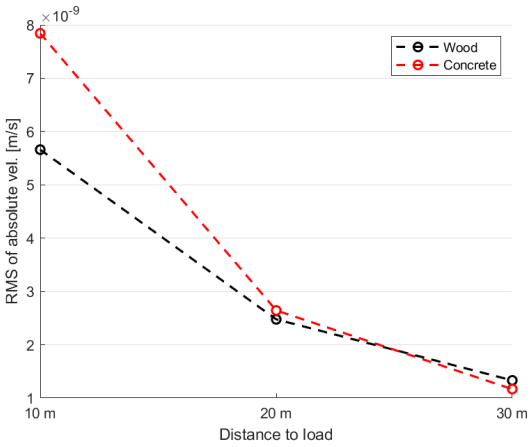

Figure 5.23: Comparison of RMS of velocity.

5.2.2 Train speed

The train speed is the only parameter which does not have a counterpart in the parameter studies for a stationary load. Studying Figures 5.25c and 5.25d, the impact of train speed is high. A doubling of velocity from 60 km/h to 120 km/h results in a 108% RMS of velocity increase for the wooden building and a 104% increase for the concrete building.

Examining the building amplification in Figures 5.25e and 5.25f shows that the amplification in the 1-8 Hz range is similar for all train speeds. At higher frequencies, some inconsistencies appear. At 39 Hz, a peak in amplification appears for a train speed of 120 km/h, which does not appear for the other speeds. For speeds of 60 and 90 km/h

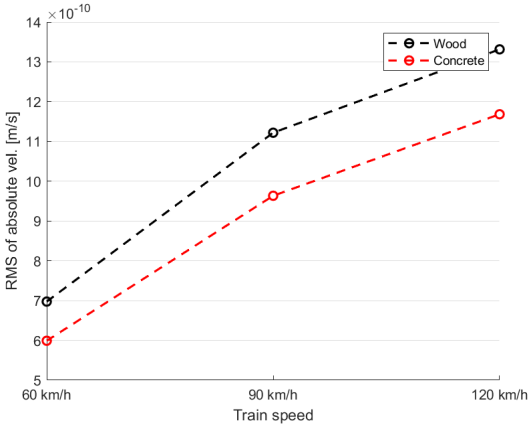

Figure 5.24: Comparison of RMS of velocity.

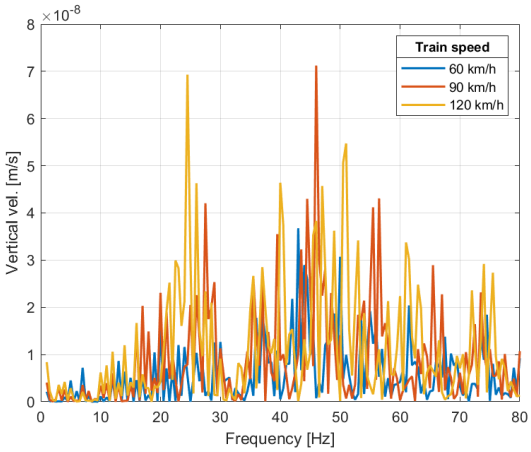

(a) Velocity in the wooden building.

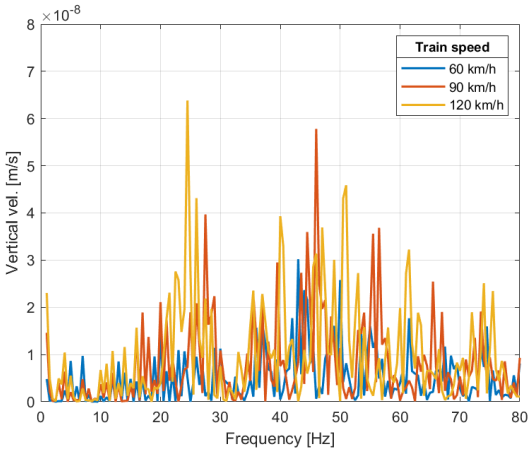

(b) Velocity in the concrete building.

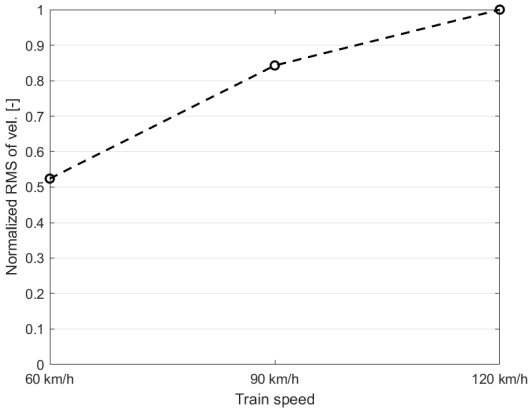

(c) Normalized RMS of velocity in the wooden building.

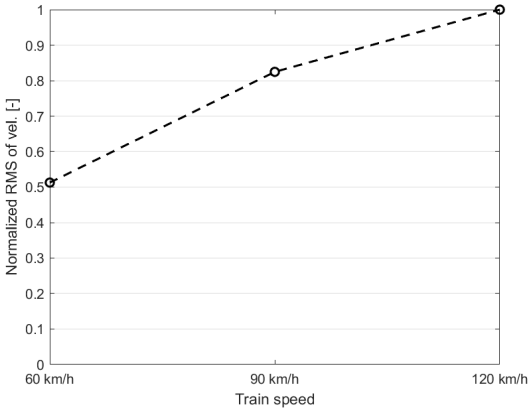

(d) Normalized RMS of velocity in the concrete building.

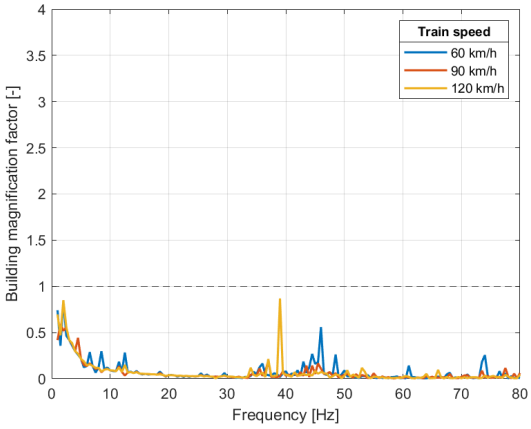

(e) Building amplification in the wooden building.

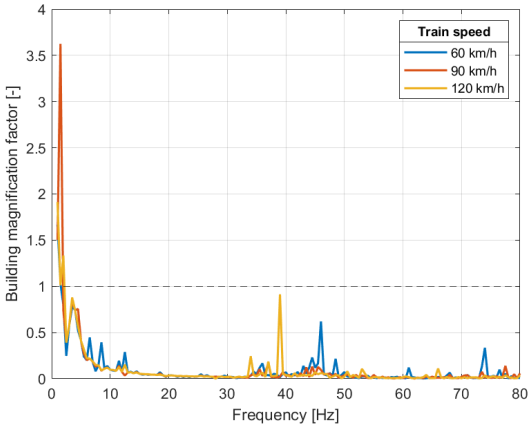

(f) Building amplification in the concrete building

Figure 5.25: Results of the parameter study of the train speed.

a increase in amplification is found in the wooden building at around 45 Hz. This increase is not observed when the train speed is 120 km/h. There is a corresponding peak in the concrete building, but only for a train speed of 60 km/h.

Comparing the vibration response in the two buildings in Figure 5.24 shows that there is no significant difference in the effect on each buildings vibration level. Moreover, the wooden building performs worse than the concrete building at all speeds.

5.2.3 Cross section of pillars

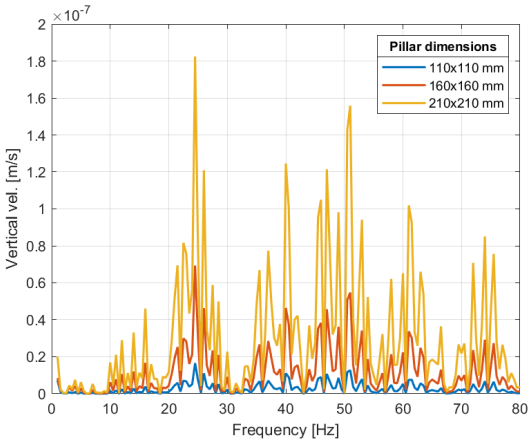

(a) Velocity in the wooden building.

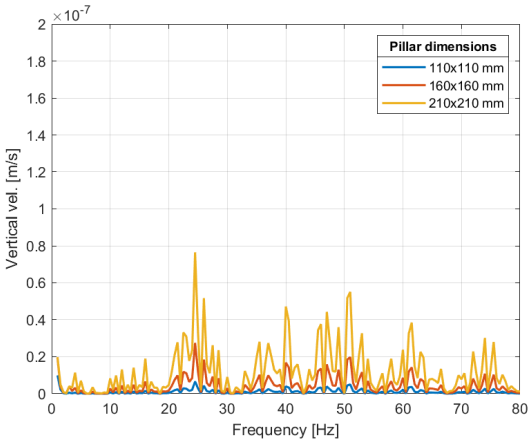

(b) Velocity in the concrete building.

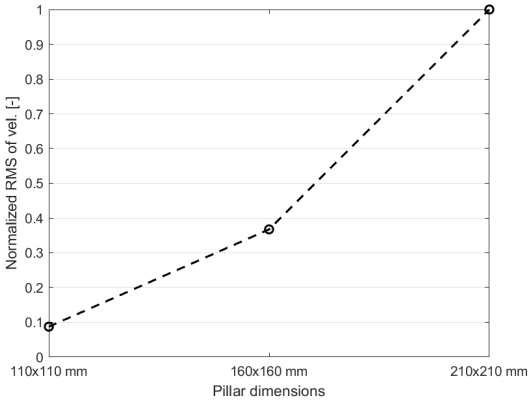

(c) Normalized RMS of velocity in the wooden building.

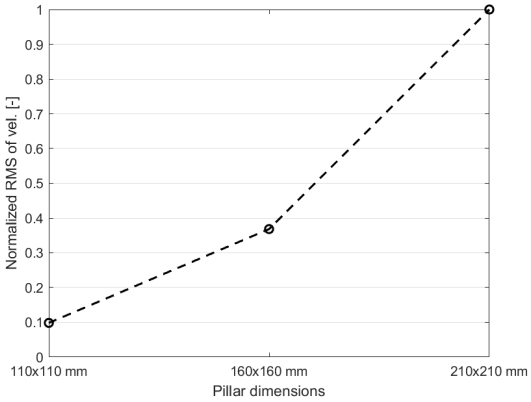

(d) Normalized RMS of velocity in the concrete building.

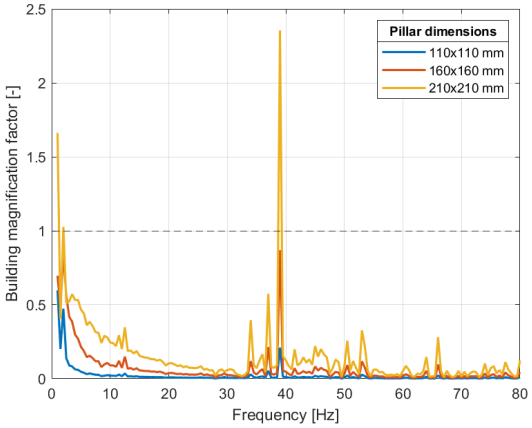

(e) Building amplification in the wooden building.

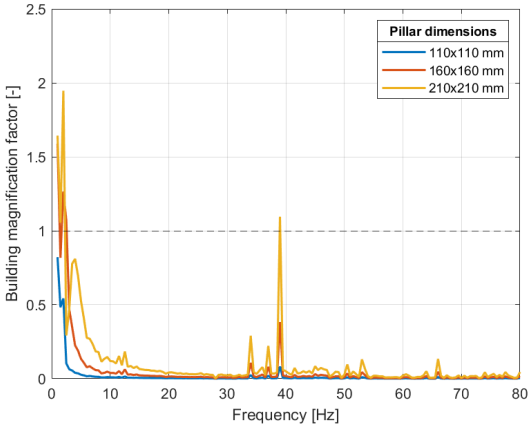

(f) Building amplification in the concrete building

Figure 5.26: Results of the parameter study of the pillar cross section.

Note that the results for the concrete building can not be directly compared to the corresponding parameter study for a stationary load, as the pillar dimensions are not the same.

The pillar dimensions has a large impact on the measured vibrations within the building, as can be seen in Figures 5.26c and 5.26d. Studying the smallest cross section,

the RMS values are only 9 % and 10 % of those found for the largest cross section in the wooden building and concrete building, respectively. This is a significantly larger impact than for the corresponding parameter study for a stationary load when considering the wooden building. The pillar dimensions does not seem to impact at which frequencies building amplification occurs in Figures 5.26e and 5.26f, but does seem to impact the magnitude of the amplification. This implies that the pillars does not impact the bending modes but rather the vibration transmission into the building.

Comparing the two building types against each other in Figure 5.27 shows that the impact of changing the cross section is higher in the wooden building than the concrete building.

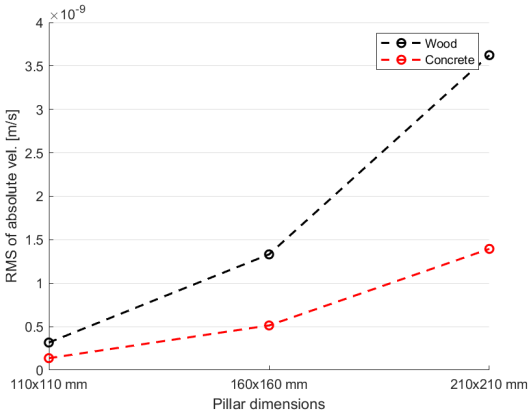

Figure 5.27: Comparison of RMS of velocity.

5.2.4 Damping

Results for the wooden building are presented. The increase in damping from 0.02 to 0.10 results in a roughly fourfold increase in the measured vibrations as seen in Figure 5.28b. The change appears to be linear, however, more data points would be required for this to be conclusive.

The building amplification factor in Figure 5.28c shows a similar behavior as for the results of the study of a stationary load, that when the building amplification is high a higher damping results in lower amplification, and when the soil movement is dominant the higher damping results in higher vibration transmission. The last point is also supported by Figure 5.28a, however the effect on the vibration levels during high building amplification is not clear in this graph. The results from studying the moving load does not contradict the hypothesis explaining the behavior presented in Section 5.1.8.

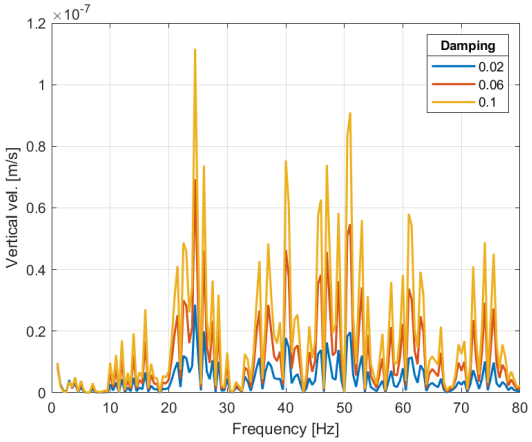

(a) Velocity in the wooden building.

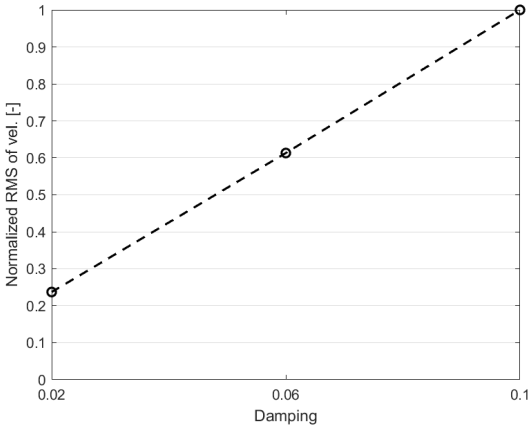

(b) Normalized RMS of velocity in the wooden building.

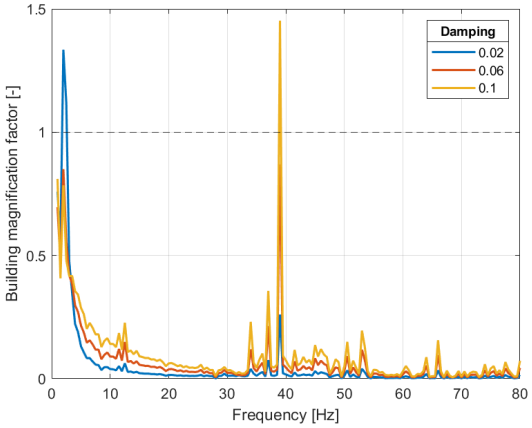

(c) Building amplification in the wooden building.

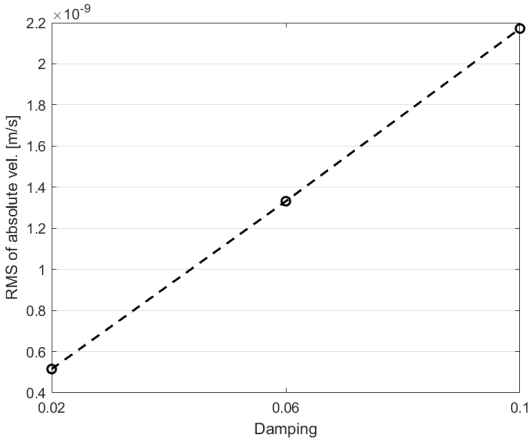

(d) RMS of absolute velocity in the wooden building.

Figure 5.28: Results of the parameter study of the structural damping.

5.2.5 Soil

The results for the wooden building are presented here. As with the corresponding study of a stationary load, the Matching wood type soil produces vibration responses much higher than the two other soil types. Examining Figures 5.29a and 5.30a the response is however highest in the 1-16 Hz range, and lower than the two other soil types for most other frequencies.

The building amplification factor in Figure 5.29c varies greatly depending on the soil types. Each type has large amplification peaks at different frequencies, with the exception of the 1-5 Hz range where the resonance in the building is active. This implies that the transmissibility of vibrations from the soil varies not only on the building conditions, but also the soil conditions. However, there is a possibility that a higher density of observation frequencies might reveal other amplification peaks and behaviors.

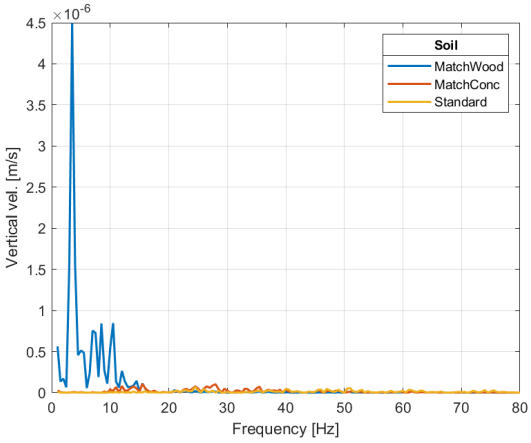

(a) Velocity in the wooden building.

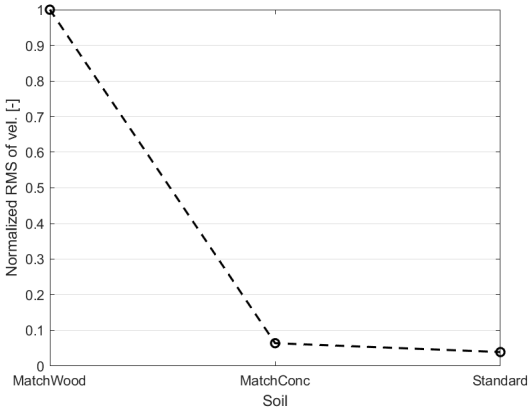

(b) Normalized RMS of velocity in the wooden building.

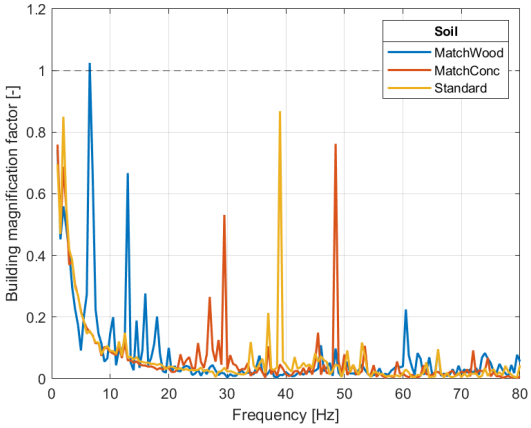

(c) Building amplification in the wooden building.

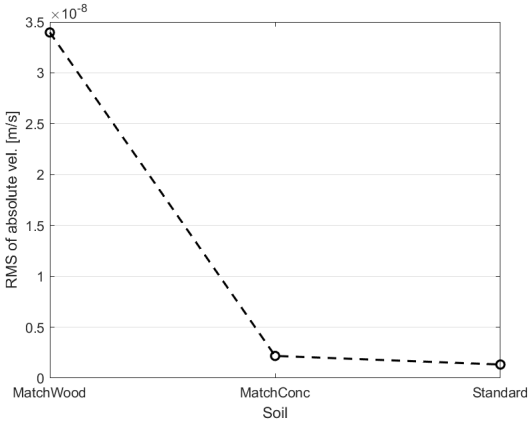

(d) RMS of absolute velocity in the wooden building.

Figure 5.29: Results of the parameter study of different soil types.

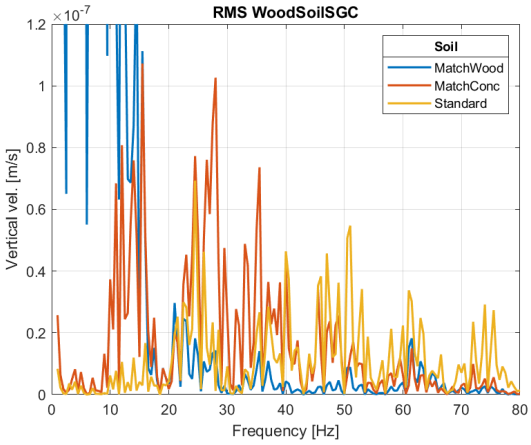

(a) Upscaled version of Figure 5.29a.

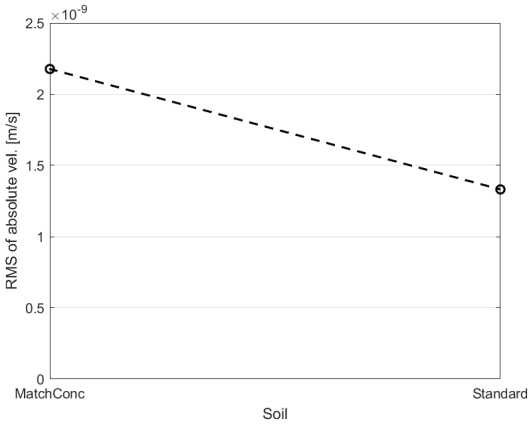

(b) Upscaled version of Figure 5.29d.

Figure 5.30: Upscaled Figures for examining the Matching concrete and Standard types of soil.

6 Discussion

This dissertation has established a framework for analyzing building vibrations within parameter studies using semi-analytical models in both a stationary and mixed FOR. These models allow the simulations to run with a significantly lower computational cost compared to the commonly used FE method, while still allowing for much of the same flexibility that the FE method has. The soil model is able to simulate three dimensional wave propagation and has the ability to couple the soil to FE structures, cavities and rigid elements. For the *GCity* program, total runtime for one parameter was around 10 minutes, while for the *SubGCity* program the runtime for one parameter was around 120 minutes. This is highly dependant on the computer used, as both programs allows for parallel computing. However, the models used are entirely based upon using Matlab code to generate the soil, track and building models, as well as for evaluating the results. While coupling to external FE programs is possible, there is currently no established method of doing so and would require extensive knowledge about the programs code structures. Developing a framework for simpler input and results analysis would greatly benefit the accessibility of the program.

By using four different evaluation metrics, both the overall impact of a parameter and the behavior of the building-soil system for each parameter may be interpreted. The use of a building amplification factor has been useful to investigate the impact of building resonance on the overall vibration levels. It has shown that the effect of building resonance on overall vibration levels is small compared to the transmission of vibrations from the soil. Furthermore the effect of resonance is mostly limited to the sub 15 Hz frequency range. Changing the soil parameters were shown to have a significant impact on the measured vibration levels. By attempting to match soil large frequency responses to the buildings natural frequencies the hypothesis was that it would induce higher building amplification amplitudes. This was however not the case for the studied buildings, and as the soil seemingly did not have a significant effect on the amplification amplitudes.

The building model examined in this dissertation is simplified. As it only contains the basic structural elements with no stabilizing system, walls or furnishings, the direct application of the results to real world buildings should be approached with care. Furthermore the parameter study of a stationary load only considers the effect of a unit load propagating from one position at each frequency. When examining realistic vibration sources, the loading will occur with different magnitudes at different frequencies, and will often not be stationary but moving, such as with railway vibrations. This means that knowledge of the vibration source and its excitation frequencies is required to apply the results on real world conditions. This is exemplified when comparing the two respective parameter studies of the effect of distance to the track in Sections 5.1.5 and 5.2.1. Here it was noted that the concrete building outperformed the wooden building at all distances when affected by the stationary load, but when the moving load was analyzed the results instead indicated that the wooden building outperformed

the concrete building at short distances to the track. The exact reason for the discrepancy in the two results can not easily be determined due to the complexity of the train and track system causing the moving load, but it can be reasoned that it is some combination of the different load magnitudes at different frequencies, the variability of the train's distance to the building and the changing angles that the soil waves hits the building from. These factors does not however mean that the stationary load case can not be applied to any more realistic conditions. For both the studies of pillar cross section and damping the conclusions drawn from the stationary load case in Sections 5.1.7 and 5.1.8 seems to also apply when examining the moving load in Sections 5.2.3 and 5.2.4.

The results showing that higher structural damping causes higher vibrations are particularly interesting. This parameter has to the author's knowledge only been studied once in the context of coupled soil-building vibrations, using a two-dimensional plain stress model with a slab foundation. In this study it was found that higher damping resulted in lower vibrations levels [4]. Why the results differ from that of this study is unclear, but as noted there are several differences in both modelling approach and building structure which might impact how the damping affects the building vibrations. It is important to note that damping in real structures is significantly more complicated than a single value representing all material damping. Joints, walls, furnishings and other building elements may have a significant impact on the damping behavior of a building. It is also not known if higher damping resulting in higher vibrations is limited to structural systems using pillars, beams and plates, or if it applies also applies to other systems, e.g. structures using bearing walls or trusses.

In the moving load case, a single vehicle was used as a load source. This is however uncommon on real railways. Most railway traffic has several vehicles that may vary in weight and properties, and this should be accounted for when examining real conditions. For the comparative parameter study in this dissertation using one vehicle was considered acceptable to reduce computation cost.

A key investigation of this dissertation was the comparison between two similar buildings using different materials. A common view is that concrete buildings are superior to wooden buildings in high vibration environments. The parameter studies conducted has shown that the examined wooden structures generally have higher vibration levels compared to examined concrete buildings, but that there were exceptions where the wooden building outperformed the concrete one. These exceptions were in the cases of similar structural damping for both buildings, a building placed on soft soil and a building placed very near a railway track.

No comparison to real vibration criteria such as VC-curves or ISO guidelines was conducted in this master's dissertation. For the stationary load case the use of a unit load means that the measured RMS values are not valid for uses other than comparison within the parameter study. For the moving load case, the comparison to real vibration criteria is not valid even though the loading is realistic, as the building model is simplified and only considers a single vehicle on a single track model, the comparison would not yield any useful information for the purposes of this dissertation.

7 Conclusions

This dissertation aimed to further the understanding of wooden and concrete buildings exposed to railway induced comfort vibrations. The main conclusions and limitations of the work are as follows:

- Using a semi-analytical soil model coupled to a railway track and FE building, the calculations could be made at a much smaller computational cost compared to the more commonly used FE method.
- The parameter studies found that for the examined buildings and soil types, vibration levels were generally highest in the wooden building, with the exception of buildings with similar structural damping, buildings placed on soft soil and buildings placed very near a railway track.
- When comparing the stationary load cases to the moving load cases, it was found that the results of a steady state analysis does not always agree with the results when considering a moving train load, but that in general conclusions drawn from the steady state analysis applied when considering a moving load.
- A major finding of the parameter studies was that a higher structural damping resulted in higher vibration levels in the buildings. This contradicts the results of the only known previous study of damping in buildings exposed to external vibrations.
- When examining the resonance behavior of the buildings, it was shown that the resonance of the examined building had a small effect on measured building vibrations compared to the transmission of vibrations from the soil. Furthermore, matching a soil's large response frequency to a natural frequency of the building showed no significant effect on vibration levels.

8 Suggestions for future work

There are several avenues for future works to investigate the methods used and results gained from this dissertation. These are suggested as follows:

- An investigation of the effect of other parameters such as foundation types, building footprint, rotation of the building, and the use of other structural systems. This could provide additional insight into how other types of building systems responds to railway vibrations.
- Examining the cause of the result that higher damping results in higher vibration levels, and how this result can be further applied to building design.
- An application of the model to investigate a more complicated FE-building model to examine how the models may be applied to more realistic scenarios and examine the validity of the results reached for a simple building model. By coupling the model to a more refined FE-program than the built in one, or using stiffness and mass matrices made in other programs, more accurate and complex behaviors might be uncovered.
- Using more powerful computer systems to investigate the effect on higher frequency vibrations and noise. A higher frequency density might also be used with more computing power.
- Investigating the effect of different rail profiles and train types on building or free field vibrations.
- As the models support cavities and barriers, the effect of urban environment factors like sidewalks, streets and trenches might be investigated. This also allows for the investigation of other types of railway vibration sources, such as subways and trains in tunnels.
- Calibrating the computational model to field measurements.

Bibliography

[1] Rickard Torndahl and Tobias Svensson. "Methodology for analysis of traffic-induced building vibrations". Master's thesis. Lund University, 2017. DOI: http://lup.lub.lu.se/student-papers/record/8919855/file/8921838.pdf.

[2] Peter Persson and Lars Vabbersgaard Andersen. "Efficient finite-element analysis of the influence of structural modifications on traffic-induced building vibrations". English. In: *Numerical Methods in Geotechnical Engineering IX*. Ed. by António S. Cardoso, José L. Borges, Pedro A. Costa, António T. Gomes, José C. Marques and Castorina S. Vieira. Vol. 2. 9th European Conference on Numerical Methods in Geotechnical Engineering, NUMGE 2018 ; Conference date: 25-06-2018 Through 27-06-2018. CRC Press, 2018, pp. 1557–1564. ISBN: 9781138544468.

[3] Juan Negreira Montero. *Vibration Analysis of Underground Tunnel at High-Tech Facility*. Master's thesis. 2010. DOI: http://lup.lub.lu.se/student-papers/record/3566969/file/3957096.pdf.

[4] Alfred Johansson. "Structural effects on externally induced building vibrations". Master's thesis. Lund University, 2018. DOI: http://lup.lub.lu.se/student-papers/record/8963988/file/8963989.pdf.

[5] P. Persson, K. Persson and G. Sandberg. "Numerical study on reducing building vibrations by foundation improvement". In: *Engineering Structures* 124 (2016), pp. 361–375. ISSN: 0141-0296. DOI: https://doi.org/10.1016/j.engstruct.2016.06.020.

[6] M. Villot, P. Ropars, P. Jean, E. Bongini and F. Poisson. "Modeling the influence of structural modifications on the response of a building to railway vibration". In: *Noise Control Engineering Journal* 59.6 (2011), pp. 641–651. DOI: 10.3397/1.3633330.

[7] J. Malmborg, O. Flodén, P. Persson and K. Persson. "Numerical study on train-induced vibrations: A comparison of timber and concrete buildings". In: *Structures* 62 (2024), p. 106215. ISSN: 2352-0124. DOI: https://doi.org/10.1016/j.istruc.2024.106215.

[8] Zi-Yu Tao, Chao Zou, Guang-Rui Yang and Yi-Min Wang. "A semi-analytical method for predicting train-induced vibrations considering train-track-soil and soil-pile-building dynamic interactions". In: *Soil Dynamics and Earthquake Engineering* 167 (2023), p. 107822. ISSN: 0267-7261. DOI: https://doi.org/10.1016/j.soildyn.2023.107822.

[9] Persson, Peter and Andersen, Lars Vabbersgaard and Persson, K. and Bucinskas, Paulius. "Effect of structural design on traffic-induced building vibrations". In: Procedia Engineering 199 (2017), 2711–2716. ISSN: 1877-7058. DOI: {10.1016/j.proeng.2017.09.577}.

[10] Georges Kouroussis David J. Thompson and Evangelos Ntotsios. "Modelling, simulation and evaluation of ground vibration caused by rail vehicles*". In: *Vehicle System Dynamics* 57.7 (2019), pp. 936–983. DOI: 10.1080/00423114.2019.1602274.

[11] Santis Paul De Vos. *Railway induced vibration - State of the art report*. Tech. rep. International Union of Railways (UIC), 2017. URL: https://uic.org/IMG/pdf/uic-railway-induced-vibration-report-2017.pdf.

[12] Svenska Institutet för Standarder. *Vibration och stöt - Vägledning för bedömning av helkroppsvibrationers inverkan på människan - Del 1: Allmänna krav*. Standard. 1998. URL: https://www.sis.se/produkter/miljo-och-halsoskydd-sakerhet/vibration-med-avseende-pa-manniskor/ssiso26311/.

[13] Paulius Bucinskas. "Propagation and Effects of Vibrations in Densely Populated Urban Environments". Doctorial thesis. Aarhus University, 2020. DOI: https://doi.org/10.7146/aul.389.

[14] Jens Malmborg. "Vibrations from Railway Traffic: Computational Modeling and Analysis". Doctorial thesis. 2022. DOI: 978-91-8039-374-4.

[15] William T. Thomson. "Transmission of Elastic Waves through a Stratified Solid Medium". In: *Journal of Applied Physics* 21.2 (Apr. 1950), pp. 89–93. ISSN: 0021-8979. DOI: 10.1063/1.1699629.

[16] N. A. Haskell. "The dispersion of surface waves on multilayered media*". In: *Bulletin of the Seismological Society of America* 43.1 (Jan. 1953), pp. 17–34. ISSN: 0037-1106. DOI: 10.1785/BSSA0430010017.

[17] Rongjiang Wang. "A simple orthonormalization method for stable and efficient computation of Green's functions". In: *Bulletin of the Seismological Society of America* 89.3 (June 1999), pp. 733–741. ISSN: 0037-1106. DOI: 10.1785/BSSA0890030733.

[18] Paulius Bucinskas. "SubGCity". (Version 2_0.7) [Source code], Unpublished.

[19] Paulius Bucinskas, Evangelos Ntotsios, David J. Thompson and Lars V. Andersen. "Modelling train-induced vibration of structures using a mixed-frame-of-reference approach". In: *Journal of Sound and Vibration* 491 (2021), p. 115575. ISSN: 0022-460X. DOI: https://doi.org/10.1016/j.jsv.2020.115575.

[20] X. Sheng, C.J.C. Jones and M. Petyt. "Ground vibration generated by a load moving along a railway track". In: *Journal of Sound and Vibration* 228.1 (1999), pp. 129–156. ISSN: 0022-460X. DOI: https://doi.org/10.1006/jsvi.1999.2406.

[21] Eugene OBrien Daniel Cantero Therese Arvidsson and Raid Karoumi. "Train–track–bridge modelling and review of parameters". In: *Structure and Infrastructure Engineering* 12.9 (2016), pp. 1051–1064. DOI: 10.1080/15732479.2015.1076854.

[22] W.L. Brogan. "Hertz impact between a surface and a mass-spring-mass system". In: *International Journal of Mechanical Sciences* 4.2 (1962), pp. 115–127. ISSN: 0020-7403. DOI: https://doi.org/10.1016/S0020-7403(62)80034-4.

Appendix A

Appendix

A.1 Free field response of the ground surface

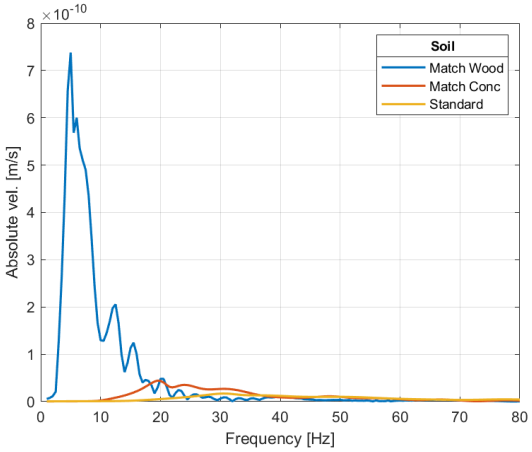

(a) Free-field response of the three types of soil.

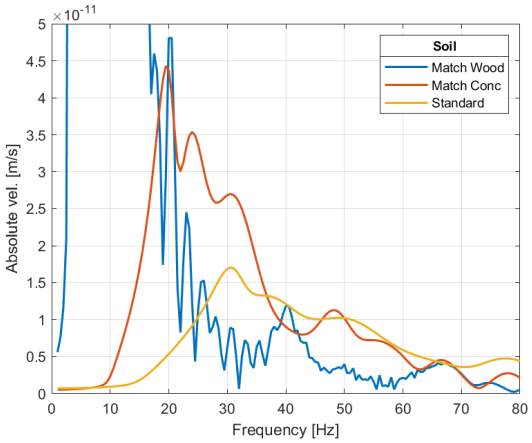

(b) Upscaled version of figure A.1a.

Figure A.1: The free-field response of the three types of soil.

A.2 Relevant eigenmodes of the buildings

A.2.1 Wooden building

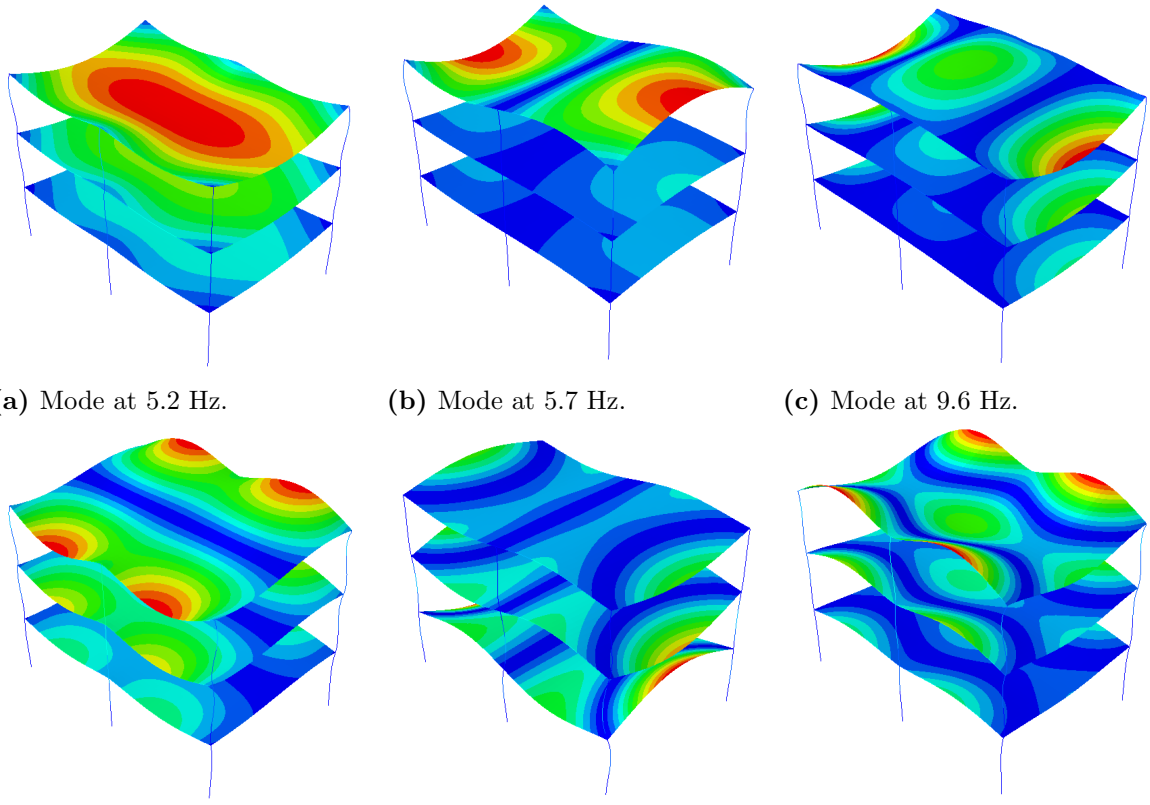

(a) Mode at 5.2 Hz. **(b)** Mode at 5.7 Hz. **(c)** Mode at 9.6 Hz.

(d) Mode at 11.2 Hz. **(e)** Mode at 14.0 Hz. **(f)** Mode at 19.0 Hz.

Figure A.2: Selection of plate bending eigenmodes of the wooden building.

A.2.2 Concrete building

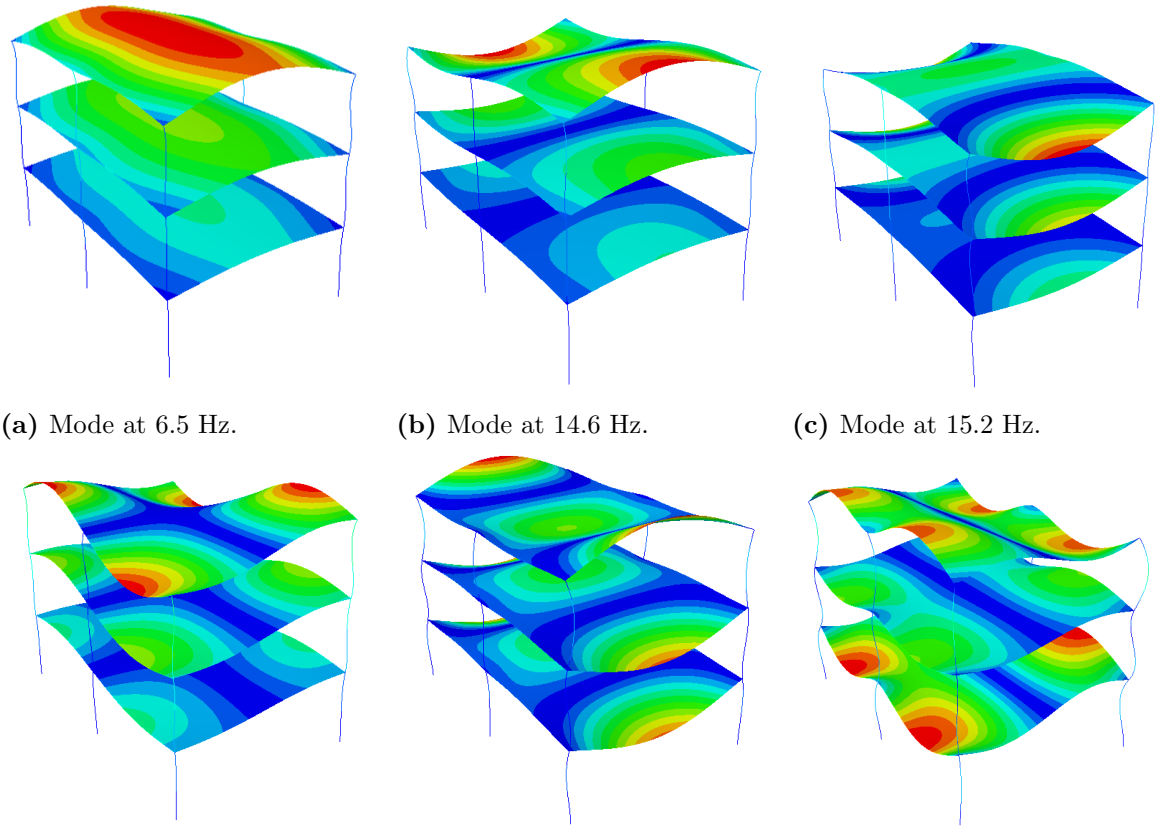

(a) Mode at 6.5 Hz. **(b)** Mode at 14.6 Hz. **(c)** Mode at 15.2 Hz.

(d) Mode at 16.8 Hz. **(e)** Mode at 17.8 Hz. **(f)** Mode at 20.6 Hz.

Figure A.3: Selection of plate bending eigenmodes of the concrete building.